frontiers | Frontiers in Molecular Biosciences

RETRACTED ON 19 FEBRUARY 2026

TYPE Original Research
PUBLISHED 24 August 2023
DOI 10.3389/fmolb.2023.1246728

Check for updates

OPEN ACCESS

EDITED BY
Yue Gu,
First Affiliated Hospital of Jilin University, China

REVIEWED BY
Deepak Balram,
National Taipei University of Technology, Taiwan
Sakshi Pareek,
Wageningen University and Research, Netherlands

*CORRESPONDENCE
Harish Kumar Dhingra,
harishdhingra2000@gmail.com
Vinay Dwivedi,
drvinay@yahoo.com
Ashish Patel,
uni.ashish@gmail.com

RECEIVED 24 June 2023
ACCEPTED 04 August 2023
PUBLISHED 24 August 2023
RETRACTED 19 February 2026

CITATION
Dadhwal P, Dhingra HK, Dwivedi V, Alarifi S, Kalasariya H, Yadav VK and Patel A (2023), *Hippophae rhamnoides L.* (sea buckthorn) mediated green synthesis of copper nanoparticles and their application in anticancer activity. *Front. Mol. Biosci.* 10:1246728. doi: 10.3389/fmolb.2023.1246728

COPYRIGHT
© 2023 Dadhwal, Dhingra, Dwivedi, Alarifi, Kalasariya, Yadav and Patel. This is an open-access article distributed under the terms of the Creative Commons Attribution License (CC BY). The use, distribution or reproduction in other forums is permitted, provided the original author(s) and the copyright owner(s) are credited and that the original publication in this journal is cited, in accordance with accepted academic practice. No use, distribution or reproduction is permitted which does not comply with these terms.

RETRACTED: *Hippophae rhamnoides L.* (sea buckthorn) mediated green synthesis of copper nanoparticles and their application in anticancer activity

Pooja Dadhwal[1], Harish Kumar Dhingra[1]*, Vinay Dwivedi[2]*, Saud Alarifi[3], Haresh Kalasariya[4], Virendra Kumar Yadav[5] and Ashish Patel[5]*

[1]Department of Biosciences, School of Liberal Arts and Sciences, Mody University of Science and Technology, Lakshmangarh, Rajasthan, India, [2]Biotechnology Engineering and Food Technology, Chandigarh University Chandigarh, Mohali, India, [3]Department of Zoology, College of Science, King Saud University, Riyadh, Saudi Arabia, [4]Centre for Natural Products Discovery, School of Pharmacy and Biomolecular Sciences, Liverpool John Moores University, Liverpool, United Kingdom, [5]Department of Life Sciences, Hemchandracharya North Gujarat University, Patan, Gujarat, India

RETRACTED

Green synthesis of nanoparticles has drawn huge attention in the last decade due to their eco-friendly, biocompatible nature. Phyto-assisted synthesis of metallic nanoparticles is widespread in the field of nanomedicine, especially for antimicrobial and anticancer activity. Here in the present research work, investigators have used the stem extract of the Himalayan plant *Hippophae rhamnoides* L, for the synthesis of copper nanoparticles (CuNPs). The synthesized of CuNPs were analyzed by using sophisticated instruments, i.e., Fourier transform infrared spectroscopy (FTIR), UV-Vis spectroscopy, X-ray diffraction (XRD), high-performance liquid chromatography (HPLC), and scanning electron microscope (SEM). The size of the synthesized CuNPs was varying from 38 nm to 94 nm which were mainly spherical in shape. Further, the potential of the synthesized CuNPs was evaluated as an anticancer agent on the Hela cell lines, by performing an MTT assay. In the MTT assay, a concentration-dependent activity of CuNPs demonstrated the lower cell viability at 100 µg/mL and IC_{50} value at 48 µg/mL of HeLa cancer cell lines. In addition to this, apoptosis activity was evaluated by reactive oxygen species (ROS), DAPI (4′,6-diamidino-2-phenylindole) staining, Annexin V, and Propidium iodide (PI) staining, wherein the maximum ROS production was at a dose of 100 µg per mL of CuNPs with a higher intensity of green fluorescence. In both DAPI and PI staining, maximum nuclear condensation was observed with 100 µg/mL of CuNPs against HeLa cell lines.

KEYWORDS

copper nanoparticles, sea buckthorn, apoptosis, ROS generation, anticancer

Introduction

Cancer arises when a cell gets through the natural barriers that prevent unchecked growth and spread (Sathishkumar et al., 2022). Evaluating medical, economic and social costs according to cause-based DALYs (Disability-Adjusted Life Years), cancer is a disease that seeks the highest expenses (Schlottmann et al., 2022). Ages up to 74 are associated with a

20.2% cancer risk. 2.09 million cases of prostate, breast and lung are the most common types of cancer diagnoses in 2018 (1.28 million cases). In India, cancer is currently the main reason for excessive medical costs, unstable finances, and rising costs before death (Kulothungan et al., 2022). Men had higher rates of lung cancer (9 PBCRs), mouth cancer (9 PBCRs), oesophageal cancer (5 PBCRs), stomach cancer (4 PBCRs), and nasopharyngeal cancer (1 PBCRs), according to population-based cancer registries. In the western and central regions, the most prevalent cancer was oral cancer, while the southern region and large cities were dominated by lung cancer. On the Indian subcontinent, men were more frequently diagnosed with oral and lung cancer (Mummudi et al., 2019; Iyer et al., 2023). The continued rise in cancer incidence, prevalence, and death underscores the necessity for modern technology to play a pivotal part in cancer therapy (Sathishkumar et al., 2022). The major challenge is that malignancies cannot be prevented by simple behavioral changes; hence technology development is necessary to improve outcomes. Viruses like the human papillomavirus (HPV) (Pareek et al., 2021) have helped the industrialized world significantly reduce the incidence of cancer (McBride, 2022). Chemotherapy is frequently used in clinics because of its simple and useful approach. Radiation and surgery are two more common cancer treatments (Pucci et al., 2019; Zhang et al., 2023).

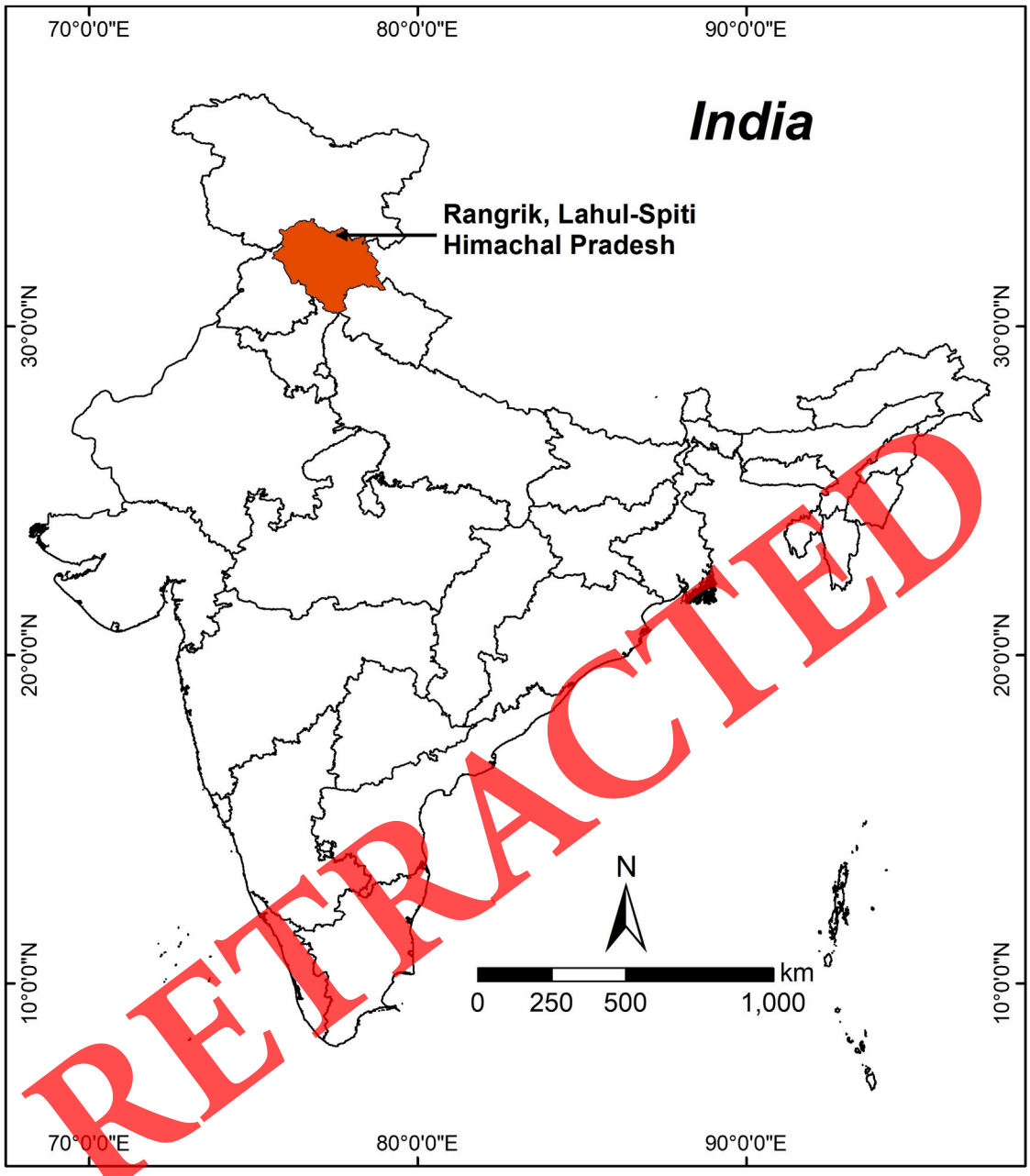
Chemotherapy, however, is associated with a number of serious drawbacks, for instance, chemotherapeutic medications are widely dispersed as well as penetrating and prone to multi-drug resistance (MDR) (Anand et al., 2023) throughout the therapy, and chemotherapy is unsuccessful at halting the growth, spread, and recurrence of tumors (Adjiri, 2016). A system to deliver the drug that integrates chemotherapy along with other therapies is required to get over these obstacles and boost the effectiveness of cancer therapies (Riley et al., 2019; Chen et al., 2022). The treatment of cancer can have negative impacts on patients' lives. Patients may experience various complications such as pain, fatigue, nausea, and diarrhoea. Chemotherapy can also result in peripheral neuropathy, a condition that causes severe nerve damage and is commonly caused by the use of anticancer drugs such as taxanes, vinca alkaloids, angiogenesis inhibitors, platinum-based therapies, and proteasome inhibitors (Loprinzi et al., 2020). Chronic chemotherapy-induced peripheral neuropathy (CIPN) has been linked to depression, ataxia, and insomnia (Loprinzi et al., 2020; Burgess et al., 2021).

Nanotechnology is a prominent scientific field that greatly contributes to the rapid advancement of technology, according to Modi et al., 2023; Ray and Bandyopadhyay, 2021; Imoisili and Jen, 2022; Modi et al., 2023). Nanoparticles (NPs) are substances whose size falls between 1 and 100 nm (Inwati et al., 2021; Choudhary et al., 2023). The field of nanomedicine involves science and technology that utilizes molecular tools and information about the human body to produce novel medications (new treatments), ailments, and tissue repair; to develop quick monitoring tests (high nanoparticles, imaging technology), throughput arrays (labels, nano biosensors, or extremely sensitive detectors) (Sebastian et al., 2022; Balram et al., 2023); to develop biopharmaceuticals (targeted medications), delivery methods, and gene delivery; and to enhance (implantable) cell function (Jagaran and Singh, 2021; Lin et al., 2021; Kim and Lee, 2022; Rhaman et al., 2022). Even though NPs could be synthesized by all three routes, i.e., chemical (co-precipitation, sol-gel, solvothermal, chemical vapor deposition, sonochemical), physical (ball-milling, physical vapor deposition), and biological (plant, bacteria, fungi, algae) (Yadav et al., 2020). Plant-mediated green synthesis of NPs is beneficial for the environment there is minimal use of hazardous and toxic chemicals. There are several pieces of literature where plants have been used for the synthesis of NPs as they are rich in flavonoids, terpenoids, and other biomolecules which may reduce the metal ions and also may act as a capping agent for the synthesized NPs. Plants are rich in various bio-active compounds such as phenols, lycopene, flavonoids, saponins steroids, tannins, vitamin C, and glycosides (Pinto et al., 2021; Shen et al., 2022; Priya et al., 2023). Most of these phytochemicals serve as stabilizing and capping agents, for the formation of NPs. NPs synthesized by plants are capped with plant-origin biomolecules which do not have any harmful effect on the patient during the application of NPs in nanomedicine or as drug delivery. But for medical applications, biologically synthesized NPs are most suitable due to their biocompatible nature (Huang et al., 2022; Singh Jassal et al., 2022). NPs synthesized biologically are intriguing and are gaining importance not only due to their high surface area but also due to their biocompatible and eco-friendly nature (Das et al., 2022; Mallikarjunaswamy et al., 2022; Rashtbari et al., 2022; Sagadevan et al., 2022).

Though there are several metallic NPs that have been used as an antimicrobial agents and anticancer activity, for instance to date, Ag, Au, Pt, Fe (0), Cu, etc., have been synthesized by using plant and their parts (Andualem et al., 2020; Sánchez-López et al., 2020; Lee et al., 2021). The majority of the metallic NPs (Ag, Au, Pt) used in the nanomedicine for anticancer activity are highly expensive, being noble metals, which restricts their application outside the laboratory (Andualem et al., 2020; Roy et al., 2021; Tuli et al., 2023). So, there is a requirement for such metallic NPs which are easily available, economical, and as effective as that of those expensive metallic NPs. One such metallic NPs is copper nanoparticles (CuNPs) which are economical and widely available (Alphandéry, 2020). CuNPs have high conductivity, in comparison to other metal NPs. Moreover, Cu is a less expensive metal as compared to noble metals like gold, platinum, and silver. CuNPs are powerful catalysts that provide great yields, have simple product separation, and may be used again (Brunet et al., 2021; Ma et al., 2022; Gobane et al., 2023). CuNPs and their oxide are mainly used for antibacterial, anticancer, and antioxidant activity (Maliki et al., 2022). It is because NPs have the ability to interact with the biological system in a variety of ways and perform a variety of tasks at the cellular level (Halbus et al., 2019).

Literature is filled with several plant-mediated syntheses of CuNPs, but very few attempts were made where the involved plants have medicinal values. So, there is a requirement for such a plant which have medicinal importance so that the synthesized NPs could get entrapped with the bioactive compounds having medicinal values. One such plant is *Hippophae rhamnoides* which is basically a hardy, deciduous shrub with a deep-rooted system which widely recognized and highly beneficial to human health and diet (Pundir et al., 2021). *Hippophae rhamnoides* can be found in different regions of Asia, with its most prevalent presence observed in the Himalayan regions spanning India, Nepal, Bhutan, and the northern regions of Afghanistan (Chen et al., 2010). These countries have used sea buckthorn to make more than ten different types of medications, which comes in variable forms like pills, pastes, powders, liquids, liniments, suppositories, films, plasters, etc (Vinita and Punia, 2018; Wang et al., 2022). This

RETRACTED



RETRACTED

FIGURE 1
Google image showing location for collection of *Hipphophae rhamnoides* L. stem.

plant has ethnomedicinal applications in different countries around for instance in Tibet its seed, fruit, and leaves are used for oedema, tissue generation, skin grafts, burning injury and cosmeceutical. In Russia, the oil of berries is used in cosmetics, skin grafts, burn injuries, etc. In Central Asia (Tajikistan and Afghanistan) it is sued for digestive disorders, hypertension, gastritis, stomach ulcers, and genital tract infections. In China, berries are used for the treatment of gastric ulcers, inflammation, radiation damage, and burns. In Turkey, its fruit and leaves are used as an antiseptic agent, for wound healing, and for ulcer treatment. While India its fruit is used as a digestive agent (Andualem et al., 2020; Lee et al., 2021; Pundir et al., 2021).

There are several cases, where the investigators have synthesized CuNPs from plants and applied them for anticancer activity. Chandraker and their team synthesized ~80 nm cubic, hexagonal, and rectangular-shaped CuNPs from the leaf extracts of *Ageratum houstonianum* Mill. Further authors assessed the antimicrobial activity of the synthesized CuNPs against *Escherichia coli* and obtained a zone of inhibition of 12.43 ± 0.23 mm (Chandraker et al., 2020).

Mali and their colleagues synthesized spherical-shaped, 2–10 nm with an average diameter of about 5 nm from the leaf extracts of *Celastrus paniculatus*. Further, the investigators assessed the antifungal activity of the synthesized CuNPs against *Fusarium*

TABLE 1 Phytochemicals present in *H. rhamnoides*.

Phytochemical tests	Qualitative analysis
Flavonoids	+
Tannins	+
Anthraquinone	-
Glycosides	-
Phenols	+
Phlobatannins	-
Anthrocynine	-
Saponins	-
Terpenoids	+
Phytosterols	-
Steroids	-
Alkaloids	+
Carotenoids	+

oxysporum which exhibited 76.29 ± 1.52 maximum mycelial inhibition (Mali et al., 2020).

Wu and their team synthesized 5–20 nm sized CuNPs using the leaf extract of the *Cissus vitiginea plant*. Further, the investigator utilized the CuNPs for the evaluation of antioxidant and antibacterial activity against pathogens causing urinary tract infections caused by *E. coli*, *Enterococcus* sp., *Proteus* sp., and *Klebsiella* sp. (Wu et al., 2020). Ghosh and their team reported the synthesis of 10 ± 1 nm sized CuNPs by using leaf extract from *Jatropha curcas* and further assessed their photocatalytic, and optical properties in addition to CT-DNA binding (Ghosh et al., 2020).

Here in the current investigation, the authors have synthesized the copper nanoparticles by using the *Hippophae rhamnoides* L plant. One of the objectives was to synthesize the copper nanoparticle by using a green approach. One of the objectives was to impart the medicinal values of the plants in the copper nanoparticles. Another objective was to characterize the synthesized copper nanoparticles by using a sophisticated instrument like UV-vis spectroscopy (UV-Vis), X-ray diffraction (XRD), Fourier transform infrared spectroscopy (FTIR), and a scanning electron microscope (SEM). One final objective was to assess the anticancer activity of the plant-mediated synthesized copper nanoparticles against the Hela cell line by MTT assay.

Materials and methods

Materials

Stem parts of *Hipphophae rhamnoides*, $CuSO_4$ (Merck, Mumbai, India), ethanol (SRL, Gujarat, India), milli-Q water (Merck, Millipore, Germany), Potassium bromide (FT-IR grade, SRL, Gujarat, India), 0.45 µm membrane filter (Millipore, India). All the chemicals were analytical grade with a purity of 98%.

Methodology

Collection of plant material sample

Hipphophae rhamnoides, and stem parts were gathered from Rangrik (Lahul-Spiti, Himachal Pradesh, India) in August 2021. The location of the Himalayan region is shown in Figure 1.

Preparation of *Hipphophae rhamnoides* plant powder

The collected stem parts were brought in to the laboratory, and cleaned thoroughly with double distilled water 2–3 times in order to remove any dust or dirt from the surface of the stem. Further, the stem was cut into several small pieces. This was followed by proper drying under a dry and shaded area at room temperature for at least 1 week in order to eliminate all the moisture from the stems. Finally, the stem was ground with the help of a mixer grinder (Bajaj, Rex 500 W, Gujarat, India) in order to obtain a fine powder. Finally, the finely ground powder was stored in an airtight reagent bottle for future applications.

Phytochemical analysis of *H. rhamnoides*

The phytochemical analysis of the powdered sample was analyzed for the identification of various compounds and biomolecules as per the standard protocol given in Table 1.

Synthesis of copper nanoparticles by *Hipphophae rhamnoides*

The synthesis of CuNPs using *Hipphophae rhamnoides* L. stem was done with some modifications (Loo et al., 2012). About 5 g of stem powder was mixed with 100 mL of double distilled water and boiled at 60°C for 10–12 min. The sample powder was filtered using a 0.45 µm and a 0.2 µm Millipore membrane filter. After fifteen minutes, utilize this filtrate (plant extract) for CuNPs biosynthesis. Of at room temperature, the biosynthesis of CuNPs was performed by mixing in 12 mL of plant extract with hundred mL of 1 mM $CuSO_4$ mixture in a beaker, then placing on a magnetic stirrer for uniform mixing. The solution color changed, indicating CuNP synthesis. Different instrumentation including X-ray diffraction (XRD), high-performance liquid chromatography (HPLC), Fourier transform infrared spectroscopy (FTIR), scanning electron microscope (SEM), UV-visible spectroscopy (UV-Vis) were used to acquire various elemental, chemical and morphological properties of the synthesized CuNPs. The color change was observed to be caused by CuNPs formation.

Characterization of copper nanoparticles

UV-visible spectroscopy

At regular intervals, a 2–3 mL sample of the mixture was collected to monitor the copper ion bio-depletion in an aqueous

RETRACTED

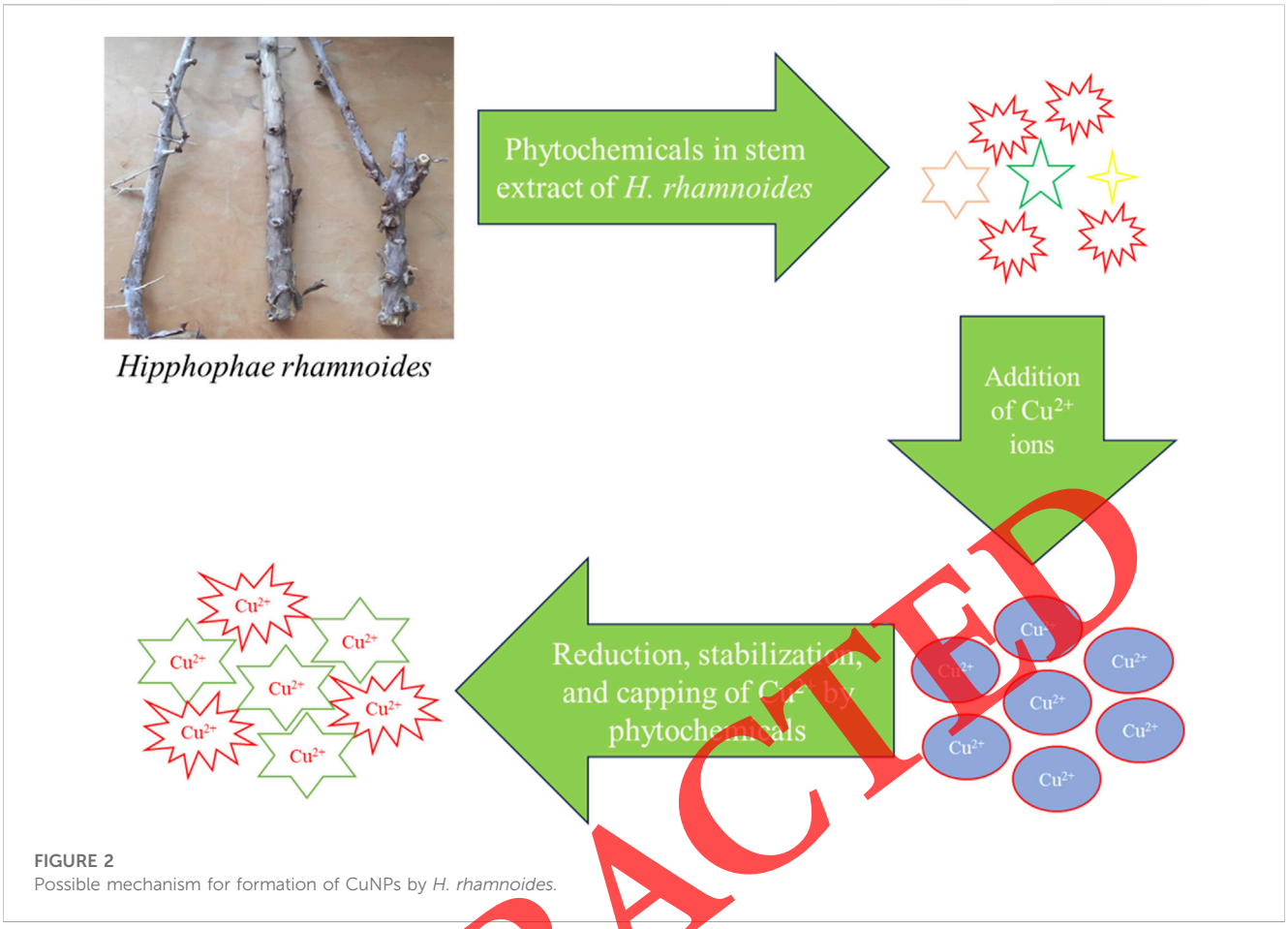


FIGURE 2
Possible mechanism for formation of CuNPs by *H. rhamnoides*.

RETRACTED

solution by using UV-vis spectroscopy within the range of 200–800 nm wavelength. If the color was darker then the collected samples were subsequently mixed with 2 mL of double distilled water (ddw) prior to scanning of the sample. The UV-vis measurement of the synthesized CuNPs was done by using Agilent, Carry 60 (United States) double-beam spectrophotometer with a resolution of 1 nm.

Fourier transform infrared (FTIR)

For, FTIR measurement, about 2 mg of CuNPs was mixed finely with 98 mg of potassium bromide (IR grade). The mixing was done with the help of a mortar and pestle. Further, the finely mixed powder was subjected to a pellet-making machine in order to obtain a pellet. Finally, the pellet was placed against a blank KBr pellet for the measurement in the range of 400–4,000 cm^{-1}, at a resolution of 1 nm by using a Perkin Elmer, Spectrum 65 instrument (United States).

Phase identification of CuNPs by X-ray diffraction (X-RD)

The crystallographic structure of CuNPs as well as phase identification was determined through X-ray diffraction pattern analysis. The CuNPs sample was analyzed by using D-8, advanced powder XRD (Bruker, Germany), in the range of two theta degrees 10°–70° with a scanning speed of 10.00° per minute and a step width of 0.02. The current was 50 mA at a voltage of 40 kV. The well-dried CuNP powder was placed in the sample holder and spectra were collected.

Morphological analysis of CuNPs by scanning electron microscope (SEM)

The surface morphology and size of the synthesized CuNPs were analyzed by the SEM-Carl ZEISS EVOR-18 (Germany). About 4–5 mg of CuNPs was sprayed with the help of a brush on the double-sided carbon-coated tape which in turn placed on an Aluminium stub. Finally, the sample loaded on aluminum stub was placed in the sample holder in the SEM, and images were taken at different resolutions with an operating current of 20 kV EHT and 8.5 mm WD.

High-performance liquid chromatography (HPLC) analysis for identifying biomolecules associated with CuNPs

In order to reveal the phytochemical associated with the synthesized CuNPs an isocratic HPLC system with a Phenomenex column was used. Different compounds migrate at varying rates depending on the column and mobile phase selected, affecting the separation degree. The mobile phase had 70% methanol, a 7.2 pH phosphate buffer solution (PBS), and ultrapure water (70:4:26 ratio). A Rheodyne syringe (Model 7,202, Hamilton) injected 20 µL of the material, and the column was kept at a constant 27°C (López-Santiago et al., 2014).

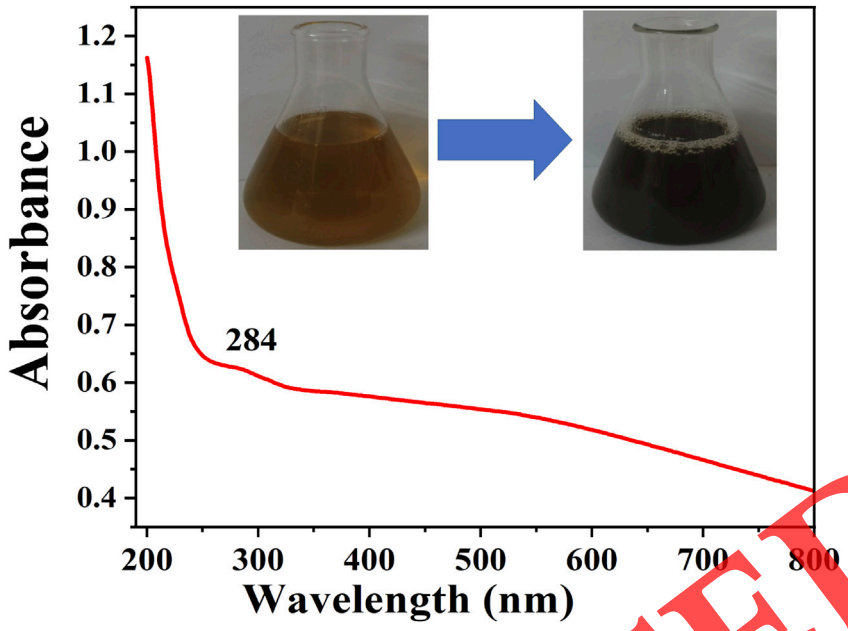


FIGURE 3
UV-Vis spectra of *H. rhamnoides* synthesized CuNPs.

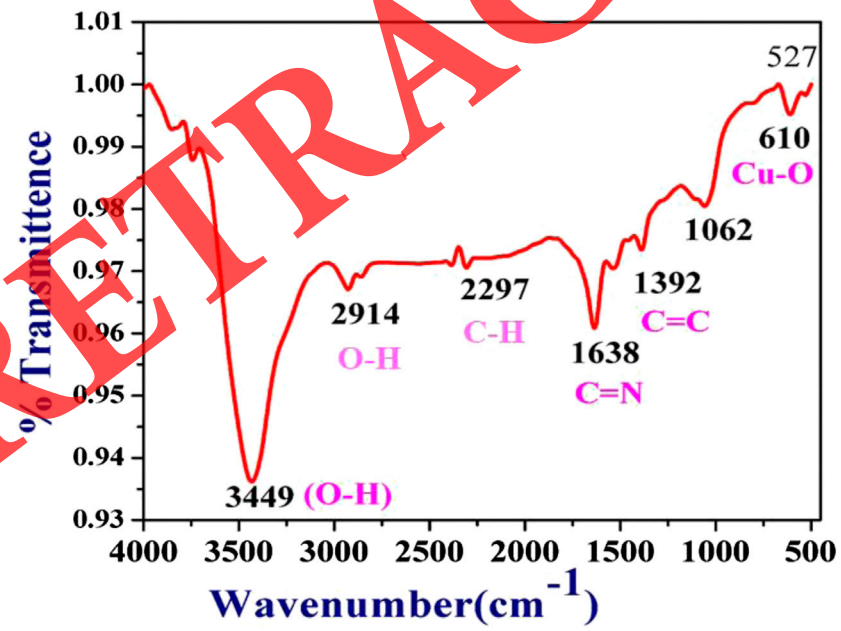


FIGURE 4
FTIR spectrum of CuNPs synthesized by *H. rhamnoides*.

RETRACTED

Anti-cancer activity of the synthesized CuNPs

MTT assay

Ten thousand cells were planted into ninety-six well plates. Followed by overnight incubation done at 37°C with 5% CO_2. The experiment was conducted using the normal cell line, L929, and the cervical cancer cell line was treated with CuNPs in different doses from 10 µg/mL to 100 µg/mL for 24 h. After the treatment, the MTT assay was incorporated, and followed by incubation for 4 h. Absorbance was measured at 490 nm, and the average % viability of cells was measured and analyzed through Student's *t*-test. The

TABLE 2 Major FTIR assignments of the CuNPs synthesized by *H. rhamnoides*.

Wavenumber (cm^{-1})	Functional group	Band in the earlier study (cm^{-1})	References
610	Cu-O (strong)	669, 480	Ghosh et al. (2020)
1,062	C-O (medium)	1,046	Ghosh et al. (2020)
1,392	C=C	–	Mohamed et al. (2022)
1,638	C≡N/OH	1,589	Ghosh et al. (2020)
2,297	C-H	2,980	Ghosh et al. (2020)
2,914	O-H (broad)	–	Wu et al. (2020)
3,449	OH	3,380	Ghosh et al. (2020)

experiment was repeated in triplicate form with a value of $p < 0.05$ considered significant. All images were taken with the help of a floid cell imaging station.

Apoptosis study

ROS generation

Following the method of Krejsa and Schieven. (2000) with some modifications, the formation ROS was determined with DCFH-DA, an oxidation-sensitive probe, via flow cytometry. Different levels of CuNPs (10 µg/mL, 20 µg/mL, 40 µg/mL, 60 µg/mL, 80 µg/mL and 100 µg/mL) were administered to HeLa cells that were grown in twelve well plates, followed by incubation with 5% CO_2 at 37°C for 24 h. Untreated cells were used as controls after washing them twice with Hanks' balanced salt solution. Subsequently, the cells were incubated in the dark with 1 mL of a working solution of DCFH-DA (10 mM) at 37°C for 30 min. The stock solution of DCFH-DA was prepared by adding 25 mM of DCFH-DA in PBS. DCFH-DA fluorescence emission was observed using a green filter after washing the control and treated cells twice with cold PBS. The green filter was used to determine the presence of ROS in the cytoplasm. All images were taken with the help of floid cell imaging station.

The evaluation of cellular apoptosis through annexin V and PI staining

The cytotoxic effects of CuNPs can induce apoptotic changes and nuclear condensation, which can be confirmed through propidium iodide (PI) staining. PI creates a bright red fluorescent complex with RNA and DNA in the nuclei of dead cells, but not in healthy cells, due to its ability to pass through damaged cell membranes (Almutairi et al., 2020).

The above process is completed in two steps: i) first is staining - wash cells with cold PBS, resuspended in 1X binding buffer, add FITC PI-annexin V, incubate for at least fifteen minutes in the dark, add 1X binding buffer, and analyzed through flow cytometry, ii) blocking–washing the cells with cold PBS, resuspension in 1X binding buffer, addition of purified recombinant Annexin V, incubation for 15 min, add FITC PI/annexin V, incubation at least for 15 min in the dark, add 1X binding buffer and analyzed through flow cytometry.

DAPI staining

The method for assessing morphological changes in the nucleus of HeLa cells due to the apoptotic effect of NPs was based on Vasanth and their team, with slight modifications. DAPI, a blue fluorescent dye that mainly stains DNA and binds to the AT-rich region of the ds-DNA, was used for this purpose. HeLa cells (fifty thousand cells/well) were planted in plates of twenty-four wells and incubated for at least 24 h. Fresh media was added, and NPs added at different levels of concentrations from (ten to hundred µg/mL), depending on the well (Vasanth et al., 2014). Incubated for another at least 24 h, then removed the media. A stock solution of 14.3 mM DAPI dye in PBS was prepared, and a working solution was made based on a concentration of 300 µM. Next, 20 µL of the working solution was poured into each and every well and allowed incubation for at least 15 minutes. Finally, the removed dye, and images were recorded by blue filter using the Floid microscopy (Invitrogen, Thermo Scientific).

The statistical analysis for the experiment involved conducting each trial in triplicate and reporting the mean value with the standard error [SE]. The standard error (SE) calculated through this formula SE = SD/$\sqrt{N}$. (SD = standard deviation, N = sample sizes.

Results and discussion

Formation of CuNPs by stem extracts of *H. rhamnoides*

The study aimed to develop CuNPs using *Hippophae rhamnoides*, the pale-yellow color turned into dark brown color. This suggests the formation of CuNPs from the stem extracts of *H. rhamnoides*. The dark color was observed due to the reduction of copper (III) to cupric ion (Cu^{+}). It happened due to the interaction between photons and conduction electrons of metal nanoparticles (Jana et al., 2016). The various phytochemicals from the stem extracts of *H. rhamnoides* were available in the aqueous medium to which an aqueous solution of Cu ions was added. All the phytochemicals reduced the oxidized Cu ions into CuNPs. Moreover, the synthesized CuNPs were stabilized and capped with several phytochemicals which are shown in Figure 2. Earlier a team led by Ghosh also showed a possible mechanism for the

RETRACTED

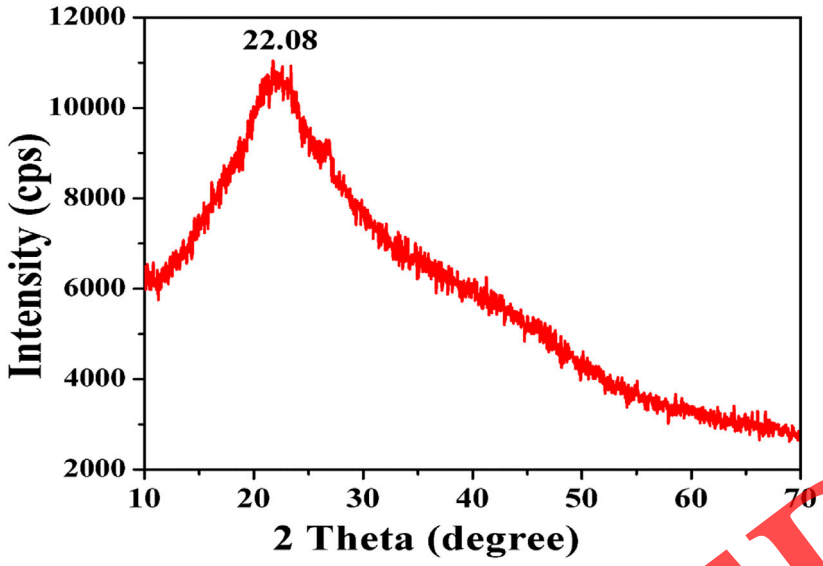


FIGURE 5
XRD pattern of CuNPs synthesized by *H. rhamnoides*.

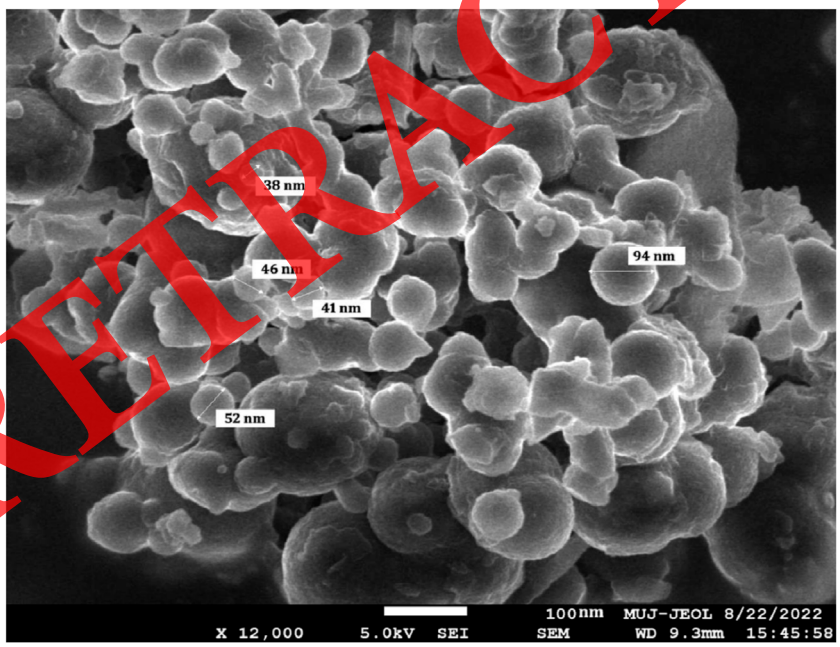


FIGURE 6
Scanning electron micrograph of CuNPs synthesized by *H. rhamnoides*.

RETRACTED

development of CuNPs by using the leaf extracts of *Jatropha curcas* (Ghosh et al., 2020). The investigators reported that the plant extracts have various biomolecules (terpenoids, flavonoids, phenols, saponin, etc.) which are responsible for the reduction of Cu^{2+} ions into CuNPs. *Hippophae rhamnoides* also have similar phytochemicals so the possible route of development of CuNPs.

Preliminary confirmation of formation of CuNPs by uv-vis

Figure 3 shows a typical UV-vis spectra of CuNPs synthesized by plant extract. The UV-Vis spectra of CuNPs arise due to the excitation of the surface plasmon resonance (SPR) phenomenon. The spectra are showing a typical absorbance peak at 284 nm which indicates the

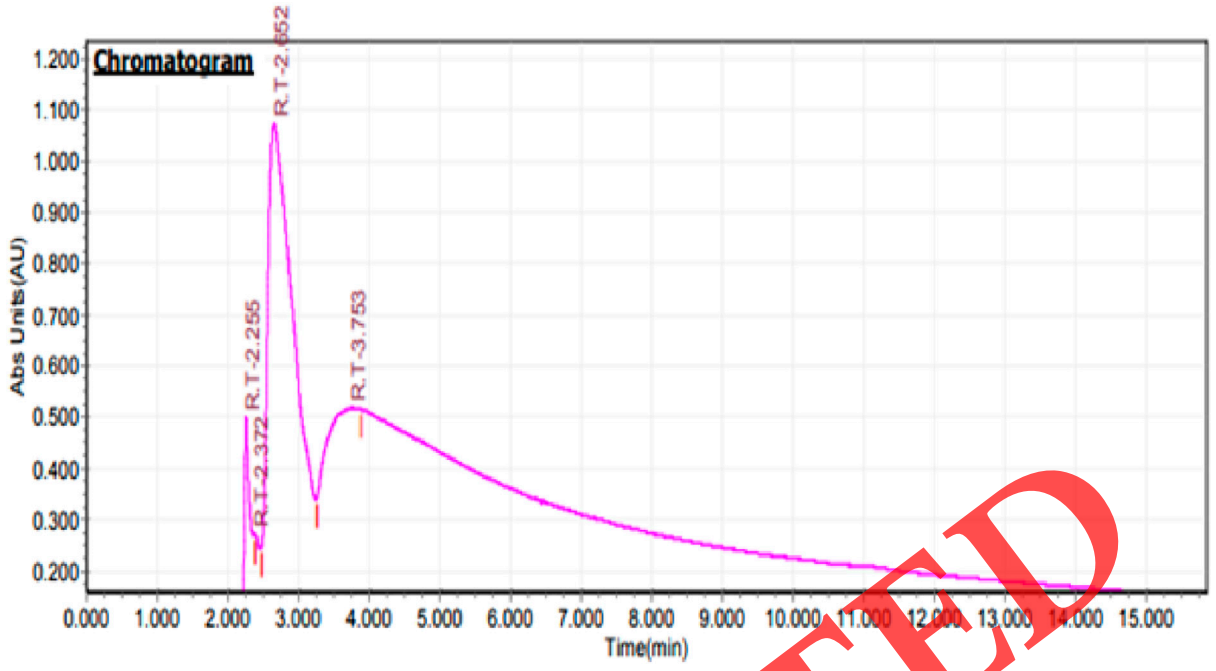


FIGURE 7
HPLC Chromatogram of CuNPs synthesized from *H. rhamnoides*.

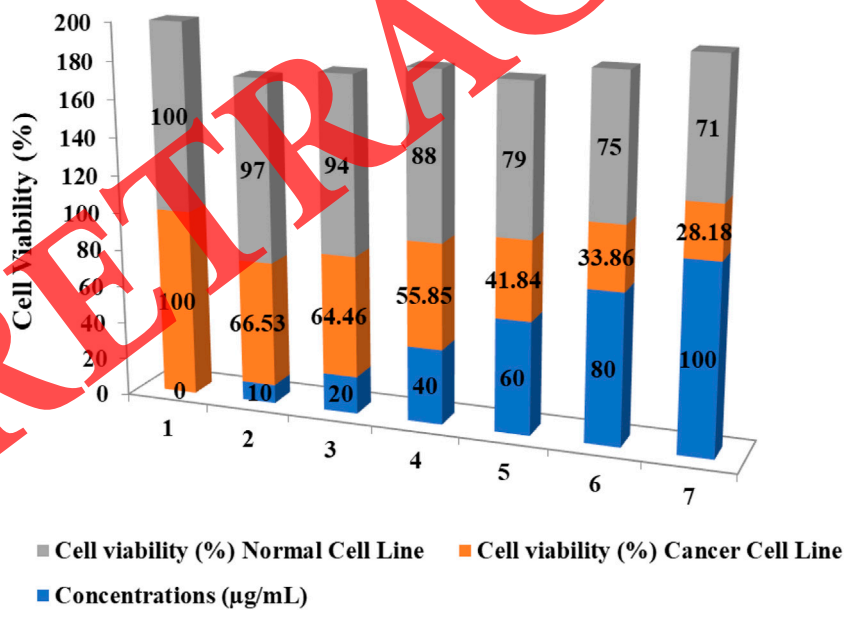


FIGURE 8
Assessing the impact of CuNPs on the viability of normal and cancerous cell lines.

RETRACTED

formation of CuNPs by using the plant extract of *H. rhamnoides*. Besides this, there was no other peak indicating the purity of the synthesized CuNPs. Previously a team led by Mali also recorded its higher absorbance is 269 nm for synthesized CuNPs from the *Celastrus paniculatus* leaves (Mali et al., 2020). Ghosh et al., obtained peaks at 337 and 266 nm for the CuNPs synthesized from the leaf extracts of *Jatropha curcas* (Ghosh et al., 2020).

Functional group identification by FTIR analysis

Typical FTIR spectra of plant-mediated synthesized CuNPs are displayed in Figure 4. The broadband signal observed at 3,449 cm^{-1} in the CuNPs material can be attributed to the -OH group, which could originate from either water molecules in the sample or other sources.

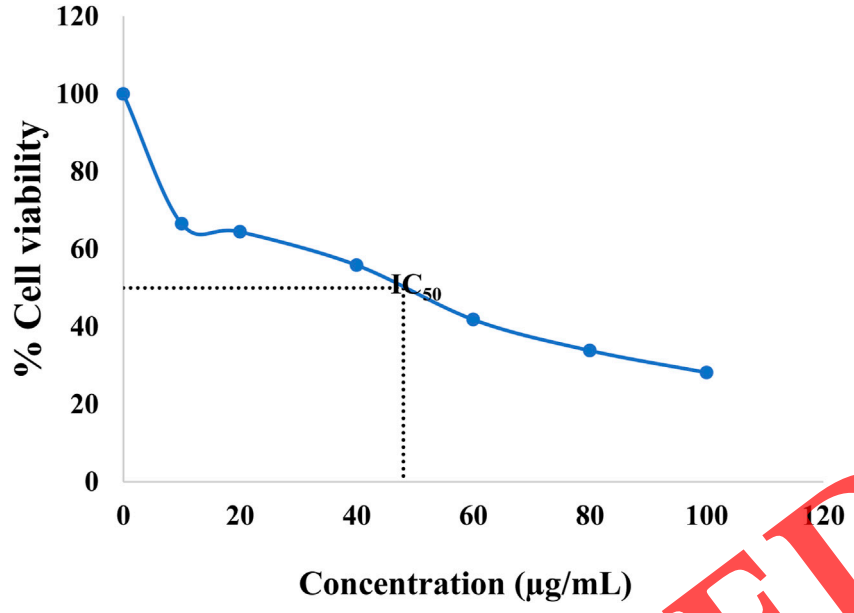


FIGURE 9
The IC_{50} of CuNPs against HeLa (cervical cancer cell line).

RETRACTED

Another band at 2,914 cm^{-1} may be due to carbon adsorbed from the atmosphere onto the surface of the CuNPs sample during analysis. The band at 2,914 cm^{-1} can also be attributed to (>CH-), 1,638 cm^{-1} (C=C stretch), 1,446 cm^{-1} (Methyl), 1,392 cm^{-1} ["iso" (doublet) or gem-Dimethyl], 1,062 cm^{-1} (1° and 2° OH in-plane bend), 816 cm-1 (C-H 1,4-disubstitution (para) of the aromatic ring (aryl) and 610 cm^{-1} (bromo compounds, (C-Br stretch) of FTIR sample containing CuNPs. The band at 610 and 527 cm^{-1} attributed to the Cu/Cu-O bond, resulting in the formulation of CuNPs along with a few CuONPs.

Copper oxide NPs (CuONPs) synthesized using *Calotropis procera,* which displayed absorption of broad peaks recorded was 3,210.44 cm^{-1} for the hydroxyl group (-OH), primarily found on the surface of CuONPs (Siddiqui et al., 2021).

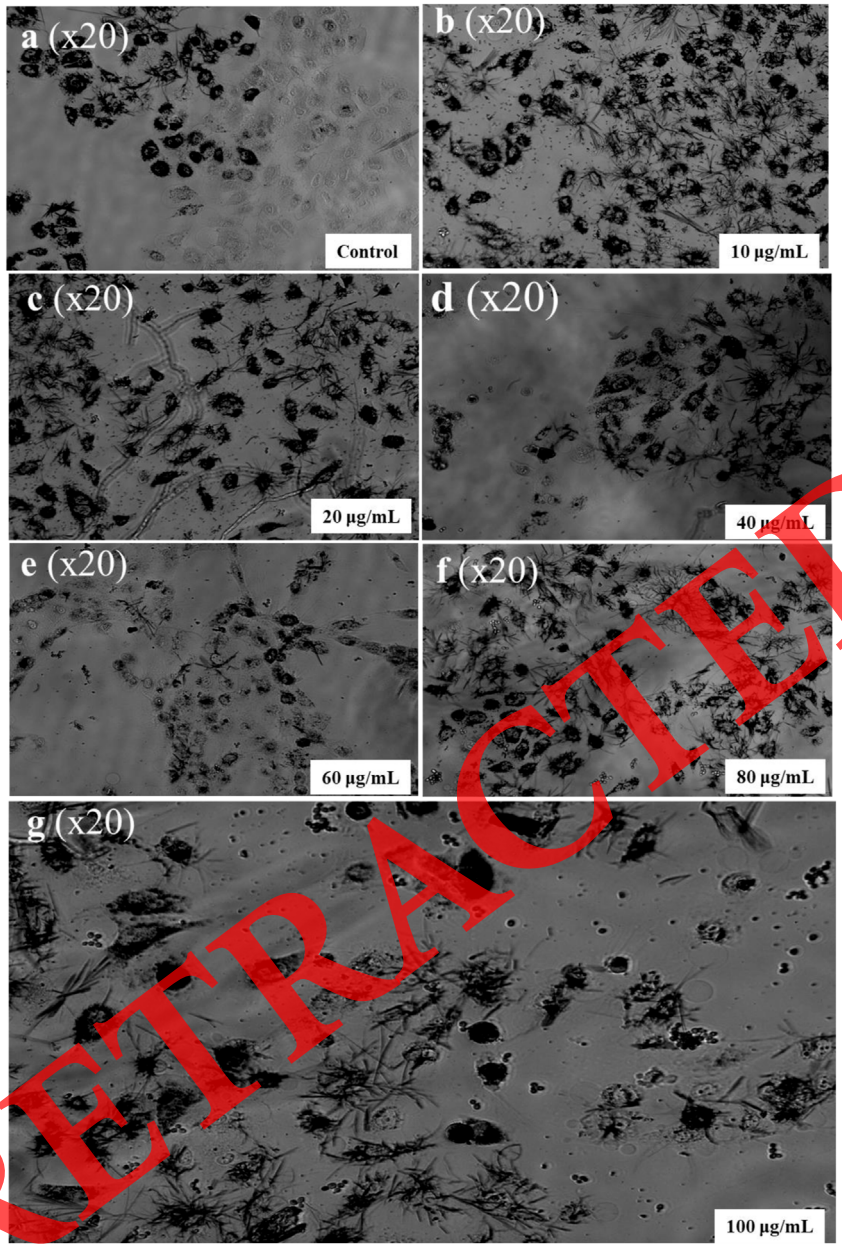
Weak absorption bands were recorded at 769.67, 862.64, 61, 985.14, and 1,072.79 cm^{-1} were linked with M-O stretching vibrations of copper oxide (M = Cu), and the mid-range peak of the spectra at 2,338.49 cm^{-1} could be attributed the availability of ambient CO_2, 2,923.88 cm^{-1} (OCH_3 stretching), 2,866.46 cm^{-1} (–CH stretching), and 1745.4 cm^{-1} (C=O stretching), 1,608.52 cm^{-1} (C=C bending) and 1,100.06 cm^{-1} (C–O stretching), which confirmed the presence of an ester group, aryl C=C group, and aliphatic C–O group respectively. From star anise, FTIR spectra connected to OCH_3 stretching and–CH stretching showed the presence of a benzene ring in the greener-formulated CuNPs (Zhang et al., 2018). Table 2 is showing the major FTIR assignments of the CuNPs synthesized by sea buckthorns and other plants.

Phase identification of the synthesized CuNPs by XRD

The XRD spectrum of CuNPs synthesized by the plant is depicted in Figure 5. The XRD pattern is showing a single peak at 22.7° which confirms the formation of CuNPs. In addition to this, a small peak is also observed at 66.4°. Furthermore, any additional peaks that were not recorded in XRD spectra indicate high sample purity. The collected data was matched with the JCPDS file 85–1,326, which is in agreement with CuNPs. Several investigators have also obtained similar peaks for the CuNPs, for instance, A team led by Wu also obtained peaks for *C. vitiginea* mediated synthesized CuNPs 35.5° and 43.2° which corresponds to lattice planes (1 1 1) and (2 0 2), respectively (Wu et al., 2020). A team led by Iliger also obtained similar types of diffraction peaks for CuNPs synthesized from extracts of Eucalyptus plant and mint leaves (Iliger et al., 2021).

Morphological analysis of the synthesized CuNPs by SEM

Figure 6 is showing spherical shaped CuNPs synthesized by *Hipphophae rhamnoides* stem. Some of the CuNPs are unaggregated while most of the particles got aggregated whose size has increased. The size of the individual CuNPs is in the range of 38 nm–94 nm while the aggregated particle size is above 100 nm. Similar, spherical-shaped were also reported by various investigators for instance a team led by Batool recorded dimensions between 80–120 nm for biogenic CuNPs using leaf extract of *Aloe barbadensis* (Batool et al., 2018). CuNPs formed by using mace extract (150–220 nm), nutmeg (170–210 nm) and star anise (210–270 nm) were noticed in the range of nanoscale (Zhang et al., 2018). Formulation of spherical shape, aggregation-free and evenly distributed bio-synthesized nanoparticle within the nano-range 40–80 nm. The formulation of CuNPs was evenly distributed with spherical in shape, within the nano ranging from 38 to 94 nm (Pugazhendhi et al., 2019; Radhakrishnan et al., 2021). The authors concluded that the shape of the developed NPs formed on the bioavailability of phytochemical components in the plant extract sample.

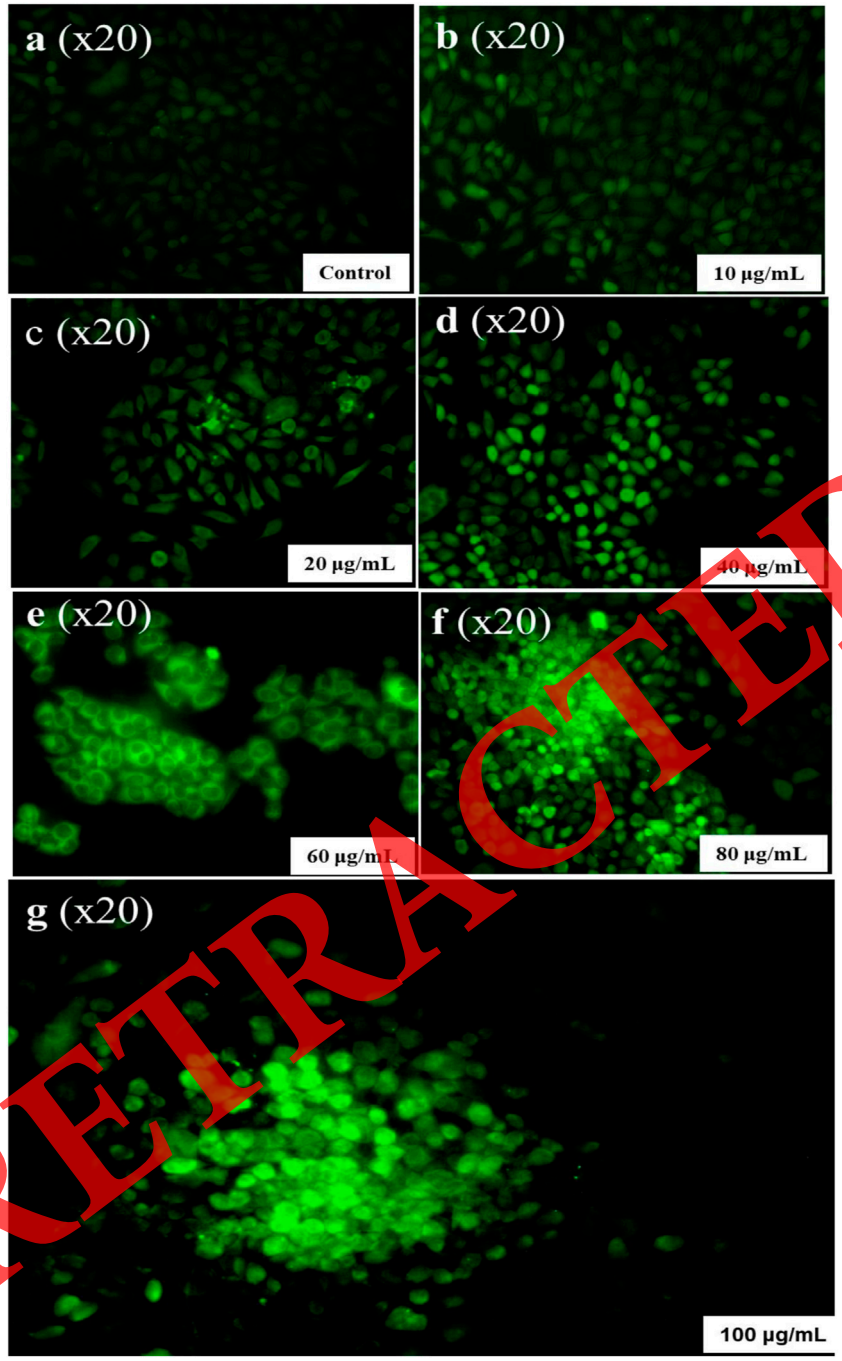


RETRACTED

FIGURE 10
Effect of different concentrations of CuNPs against HeLa (cervical cancer cell line). **(A)** Control, **(B)** 10 µg/mL, **(C)** 20 µg/mL, **(D)** 40 µg/mL, **(E)** 60 µg/mL, **(F)** 80 µg/mL, and **(G)** 100 µg/mL.

High performance of liquid chromatography for identification of biological compounds with CuNPs

HPLC was developed to explore and demonstrate the differences in bioactive chemicals between various plant sources (Ma et al., 2020). HPLC is helpful for the green synthesis of NPs particularly because of the involvement of plants as it quantifies the types of compounds present in the sample material. Here HPLC helped in the identification of biomolecules associated with the external surface of CuNPs. A sharp peak was observed at 2.652 retention time with 86.21% concentration. Investigation of *Sambucus ebulus* water extracts shows the presence of phenolic acid and flavonoid derivatives like p-coumaric acid, gallic acid, catechin, and frolic acid (Hashemi et al., 2022). HPLC application is also tested to a significant reduction in the number of active components due to ions depletion and the formulation of NPs (Kumar et al., 2019). It was concluded that the availability of bioactive constituents is the major reason for synthesizing NPs due to metal ions reduction. This research marks the initial instance where HPLC was utilized to examine CuNPs synthesized using a greener approach. To the best of our understanding, this technique has not been employed in any prior research or study to examine copper ions. Figure 7 is



RETRACTED

FIGURE 11
ROS Generation by different concentrations of CuNPs. **(A)** Control, **(B)** 10 µg/mL, **(C)** 20 µg/mL, **(D)** 40 µg/mL, **(E)** 60 µg/mL, **(F)** 80 µg/mL, and **(G)** 100 µg/mL.

showing HPLC chromatogram of CuNPs synthesized by *H. rhamnoides*.

Anticancer activity of CuNPs

MTT assay was assessed to study the cytotoxicity of formulated CuNPs The enzyme mitochondrial succinate dehydrogenase determines the reduction of MTT to formazan. (Gomathi et al., 2020). The anticancer activity of CuNPs was evaluated by evaluating HeLa cell line viability against a normal cell line (L929 cell line) at a CuNPs concentration of 0–100 µg/mL. Synthesized CuNPs demonstrated a significant negative effect on cancer cell viability as its concentration increases as shown in (Figure 8). At the highest concentration (100 µg/mL), cancer cell viability drops to 28.18%. Normal cell viability is also affected by

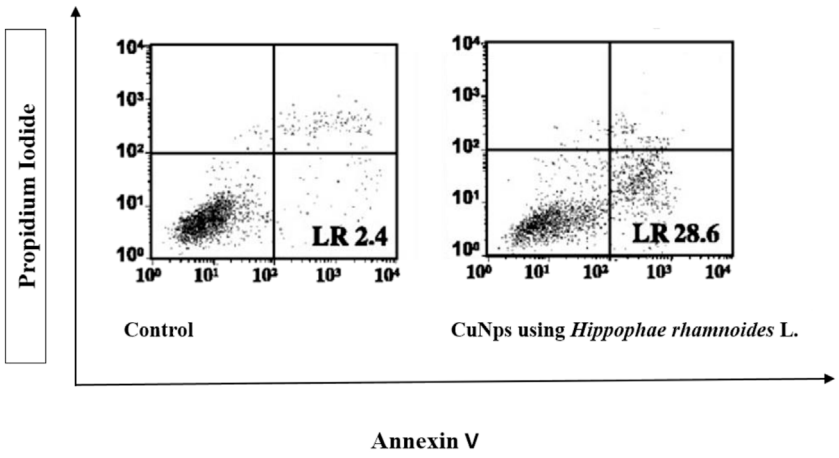


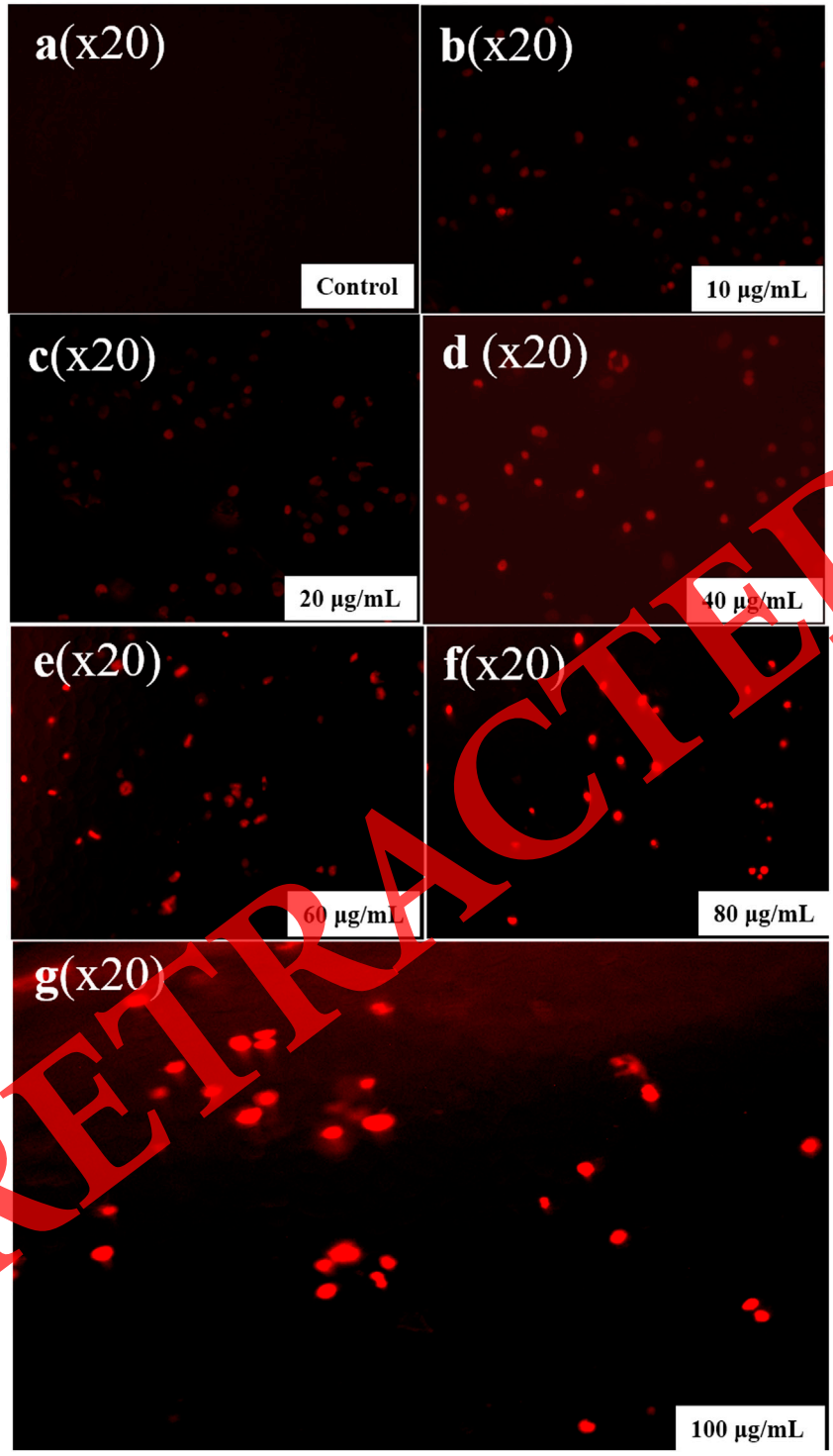
FIGURE 12
Percentage apoptosis in Hela cell lines after staining with Annexin V/PI. The cell line is treated with CuNPs using *Hippophae rhamnoides L.*

RETRACTED

the CuNPs but to a lesser extent. Even at the highest concentration, normal cell viability remains at 71%. The data shows a dose-dependent response, with higher concentrations of the CuNPs leading to a greater decrease in cell viability for both cancer and normal cells. The substance exhibits selective toxicity, preferentially targeting cancer cells over normal cells. This suggests its potential for targeted cancer treatments. Based on (Figure 9) data, the IC_{50} value is determined at 48 µg/mL. The IC_{50} value is a measure of the concentration required to inhibit or reduce the viability of a particular biological or cellular process by 50%. In this case, the IC_{50} value of 48 µg/mL suggests that the substance exhibits significant inhibitory effects on the viability of the cancer cell line at this concentration. This information further reinforces the conclusion that the synthesized CuNPs have a negative effect on the viability of the cancer cells and supports its potential for further exploration in cancer therapy. A Study led by Chung et al. (2017), reported higher cellular toxicity at a higher concentration of 500 µg/mL of CuNPs derived from *E. prostrata* leaf (Sivaraj et al., 2014). The investigators also evaluated the cytotoxic properties of copper NPs formulated with *Acalypha indica* against the MCF-7 cell line, while Biresaw and Taneja found decreased viability of the MCF-7 cell line in the manner of conc. Dependent on CuNPs synthesized by *Prunus nepalensis* (Biresaw and Taneja, 2022). Other studies have also reported significant anticancer activity of CuNPs, such as those synthesized from broccoli by Prasad and their team (Prasad et al., 2016) and from *Quisqualis indica* by a team led by Mukhopadhyay, which showed promising activity against prostate cancer cells and B16F10 melanoma cells, respectively (Mukhopadhyay et al., 2018). A team led by Gnanavel reported good inhibition of HCT-116 viability, while cell damage resulting from an increase in necrosis and cytopathic effects in the presence of NP was reported by another study (Gnanavel et al., 2017). CuNPs exhibit cytotoxicity because they interact with functional groups of proteins and with nitrogen bases and phosphate groups present in DNA within the cell (Din et al., 2017). Antitumor properties of CuNPs have been shown to have the potential in downregulating the activities of signalling proteins that are expressed inappropriately, such as cytokine-based therapies, Akt and Ras, tyrosine kinase inhibitors and DNA and protein-based vaccines against precise tumor markers that have consistent anticancer activity (Hua et al., 2021). In conclusion, CuNPs synthesized from *H. rhamnoides* L. stem could be effective as an anticancer agent. Figure 10 is showing the effect of different concentrations of CuNPs against HeLa (cervical cancer cell line).

Reactive oxygen species (ROS) evaluation

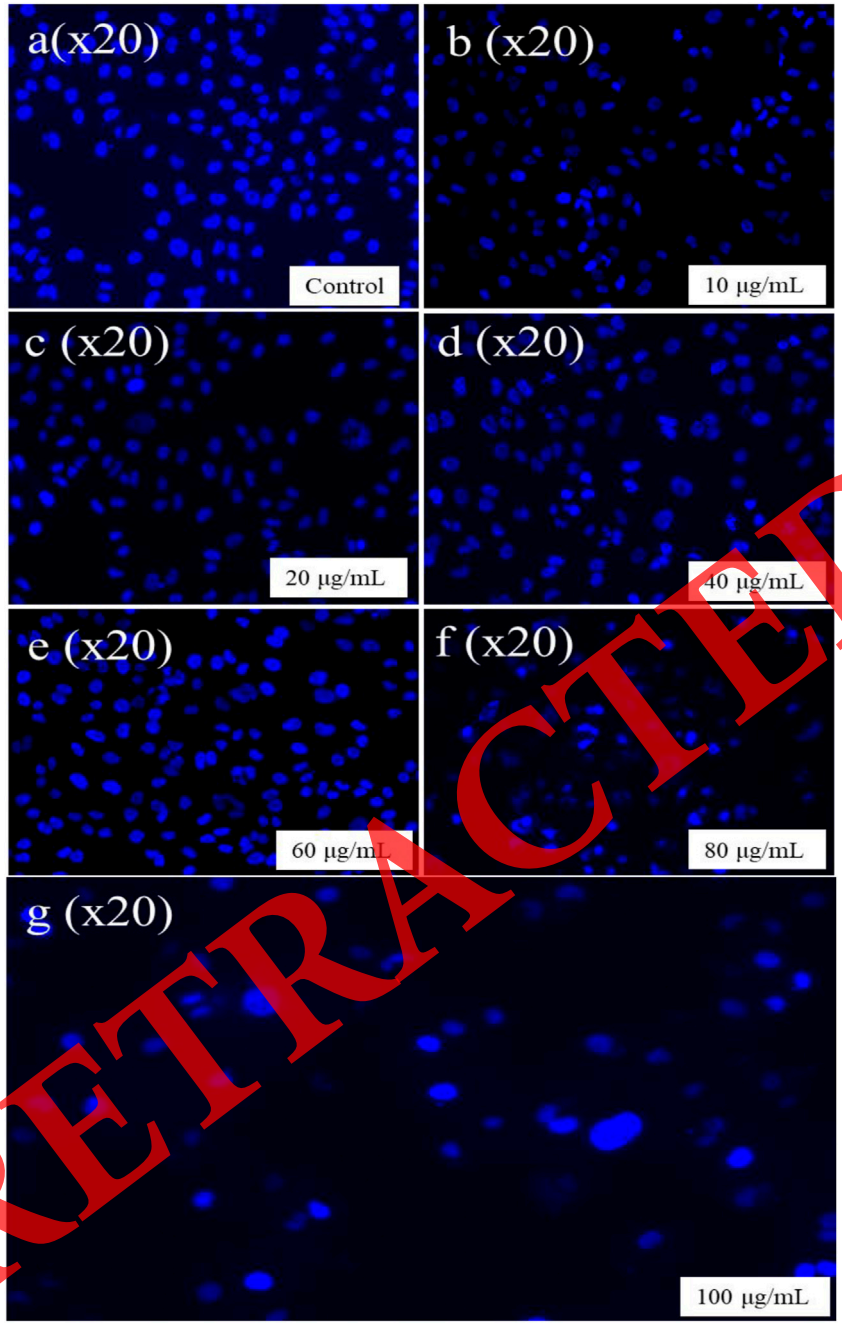
Overproduction of ROS can lead to harm to cellular health by damaging mitochondrial membranes, ultimately leading to toxicity and cellular damage (Tirichen et al., 2021). ROS are chemically harmful species that are produced naturally as by-products of metabolic activities and can damage DNA, proteins, and lipids. A team led by Aranda developed a fluorometric assay called DCFH-DA to measure the oxidative potential of NP-treated cells (Aranda et al., 2013). As per the findings of Arakha and their team, the cytotoxicity of NPs is positively correlated with ROS formation (Arakha et al., 2016). Therefore, nanoparticles can effectively suppress cancer. In this study, the authors used DCFH-DA and observed dose-dependent ROS production. Conc. of 100 µg/mL of CuNPs, ROS maximum production was recorded with a more intense green fluorescence, as illustrated in Figure 11. A disturbance between oxidants and antioxidants leads to higher basal concentrations of ROS in cancerous cells as compared to normal cells. ROS has a dual role in cell metabolism. At low to moderate levels, they act as signal transducers, activating cellular processes such as proliferation, migration, invasion, and angiogenesis. However, elevated levels of ROS can lead to harm to different cellular components including proteins, nucleic acids, lipids, membranes, and organelles, ultimately resulting in cell death. A team led by Gu evaluated the cytotoxicity activity of CuNPs synthesized by *Phaseolus vulgaris* L. against the cancer HeLa cancer cell line by inducing ROS-mediated apoptosis and mitochondrial dysfunctions (Gu et al., 2018). A team led by



RETRACTED

FIGURE 13
Propidium iodide staining in an apoptotic cell. **(A)** Control, **(B)** 10 µg/mL, **(C)** 20 µg/mL, **(D)** 40 µg/mL, **(E)** 60 µg/mL, **(F)** 80 µg/mL, and **(G)** 100 µg/mL.

Nagajyothi also found cytotoxicity activity against the HeLa cancer cell line by the generation of ROS in CuNPs formulated with dry black beans (Nagajyothi et al., 2017). A team led by Castro reported the anticancer property of green-formulated CuNPs with the help of F. *religiosa* by inducing ROS-mediated apoptosis against lung cancer cells (A459 cell line) in 2021. A team led by Pariona observed strong green-colored hyphae for *Neofusicoccum* sp., *Fusarium oxysporum, and Fusarium solani* with 0.5 mg/mL of synthesized CuNPs that represent intracellular ROS production. CuNPs-mediated anticancer action involves oxidative stressors, a buildup of ROS, genetic material fragmentation, chromosomal



RETRACTED

FIGURE 14
DAPI staining in an apoptotic cell. **(A)** Control, **(B)** 10 µg/mL, **(C)** 20 µg/mL, **(D)** 40 µg/mL, **(E)** 60 µg/mL, **(F)** 80 µg/mL, and **(G)** 100 µg/mL.

abnormality, the creation of caspases, and an increase of both intrinsic and extrinsic apoptotic pathways (Pariona et al., 2019).

Apoptosis study

Evaluation of cellular apoptosis through annexin V and PI staining

The cytotoxic effect includes apoptotic changes and the nuclear condensation can be evaluated with the help of propidium iodide staining. Propidium iodide (PI) forms a complex exhibiting high fluorescence that can be observed within the nuclei of deceased cells, indicating the presence of RNA and DNA, resulting bright red fluorescence signal. However, PI does not form this complex in the nuclei of healthy cells. This is because PI may pass through damaged cell membranes (Akintelu et al., 2020). Annexin V/PI staining showed a significant % viability of cells depletion and increment in the apoptotic cells. The lesser right quadrant shows, apoptotic cells presence. Figure 12 shows the extent of apoptotic cells after treatment with synthesized CuNPs using *Hippophae rhamnoides* L. Extent of apoptosis observed with CuNPs using *Hippophae*

rhamnoides L was 28%. Figure 13 shows red inflorescence indicating nuclear condensation observed with 100 µg/mL of CuNPs against the HeLa cell line. Images were taken and documented with the help of floid cell imaging station. Pariona *et al.*, observed red-colored mycelium of *Neofusicoccum* sp., *F. oxysporum* and *Fusarium solani,* after treatment with 0.5 mg per mL of green synthesized CuNPs. The findings indicated that the CuNPs harmed cell membranes, altering their permeability, resulting in their disintegration, and ultimately, cell death (Pariona et al., 2019). The observation of results was that NPs activate several biochemical processes that contribute to the MCF-7 cell's increased anticancer activity. Biosynthesized CuNPs by *Quisqualis indica* extract exhibited an IC_{50} reading of 102 µg/mL against the B16F10 cell line, resulting in 50% apoptotic cell death and damage. In treated cells, there was an increment in the expression of the pro-apoptotic gene Bax compared to untreated control cells. The upregulation of Bax, which is associated with p53-mediated tumor suppression, suggests that the mitochondrial pathway was stimulated during apoptosis induced by CuNPs in B16F10 cells. Caspase 3, caspase 9, and Bax expression possibly played a substantial part in mitochondrial pathway stimulation during stimulation of apoptosis by CuNPs in the cell lines of B16F10 (Mukhopadhyay et al., 2018). A team led by Bhavana, used propidium iodide staining and found that green synthesized CuONPs using leaves extract of *Vitex altissima* resulted in a good effect of cytotoxic against cells of A549 by apoptosis induction. It is also found that hyaluronic acid-hybridized, green NPs promoted apoptosis in cells through mitochondrial dysfunction, cell cycle arrest, and peroxidation of lipids (Bhavana et al., 2022).

DAPI staining

The apoptotic cell percentage with fragmented chromatin in treated cells was assessed using DAPI, a blue fluorescent dye. This assessment was used to reflect the nuclear modifications underlying apoptosis (Carneiro and El-Deiry, 2020; Lindenboim et al., 2020). This dye exhibits a commendable affinity for A-T-rich parts of DNA. In the present study maximum nuclear condensation was observed with brighter fluorescence at 100 µg/mL level of CuNPs. DAPI assay was used to confirm the apoptotic property of CuNPs (Figure 14). Asghar and their colleagues reported that in the human lung as well as breast cancer cell lines treated with CuNPs with *Dillenia indica* bark extract that have small, condensed nuclei, the number of apoptotic cells was considerably higher, implying increasing numbers of apoptotic cells with incubation at longer as compared to control cells (Asghar et al., 2020). The significance of methanol extracts apoptotic activity of leaves of *Moringa oleifera* with bright fluorescence in a concentration-dependent manner against cells of PC-3 (Khan et al., 2020). Jeronsia and their team synthesized CuNPs synthesized by *Camellia sinensis* (L.) and confirmed that the developed CuNPs have better cytotoxicity against cancer cell MCF-7 (Emima Jeronsia et al., 2019). A team led by Ramanathan synthesized CuNPs with *Syzygium alternifolium* and demonstrated their potential to suppress cancer growth by inducing cytotoxicity against the MCF-7 cell line (Akintelu et al., 2020; Waris et al., 2021; Chakraborty et al., 2022). Another similar study found that CuNPs can inhibit the growth of AMJ-13 and MCF-7 breast cancer cells (Vishnu et al., 2016). CuNPs derived from *Calotropis procera* (Aiton) extract were found to induce apoptotic destruction of BHK 21 and HeLa cell lines. Despite limited research on the effects of cytotoxic copper NPs on the HeLa cancer cell line, no prior experimental work has explored the potential anticancer and apoptotic properties of aqueous preparation CuNPs with *Hippophae rhamnoides* stems (Chowdhury et al., 2016). As a result, this study represents the first report on this topic.

A group of investigators synthesized CuNPs by coprecipitation approach which was functionalized by glutamic acid. These functionalized CuNPs were then conjugated with thiosemicarbazone (TSC), which stimulates apoptosis in breast cancer cell lines and normal cell lines (HEK293). The functionalized nanoparticles displayed an *in vitro* cell viability activity that demonstrated concentration-dependent anti-proliferative effects (IC_{50} = 133.97 µg/mL) while the IC_{50} of the functionalized CuNPs on the normal cell line was recorded at 230.2 µg/mL (Shafiei et al., 2022). A team led by Badrooh developed a spherical-shaped complex of TSC and CuNPs whose size was varying from 10 to 60 nm that can trigger the apoptosis of Adenocarcinoma gastric. The study proved that the synthesized complex proficiently depleted the augmentation of AGS cells with significantly reduced IC_{50} reading (203 µg/mL) than HEK293 (IC_{50} = 435 µg/mL) (Badrooh et al., 2022).

Conclusion

The current investigation shows that the *H. rhamnoides* have the potential to synthesize copper nanoparticles with enhanced medicinal properties. The presence of flavonoids, enzymes, and proteins helped in the bioreduction, capping, and stabilizing of the synthesized copper nanoparticles. The microscopic analysis confirmed the formation of a spherical shape particle of size 38–94 nm. The XRD helped in the phase identification with a peak at 22.8. The presence of biomolecules associated with the synthesized copper nanoparticles was confirmed by FTIR and HPLC. Concentration-dependent level decrease in cell viability was concluded in the MTT test, and the conclusion of ROS generation, DAPI, and PI staining confirmed cancerous cell apoptosis. Thus, the study suggests that CuNPs could serve as potential anti-cancer medicine in cancer treatment. One unique aspect of this investigation is that the concentration-dependent level of CuNPs is proficiently suppressed in the HeLa cancerous cells.

RETRACTED

Utilizing *H. rhamnoides* stem extract in the formulation of CuNPs represents a promising approach for eco-friendly technology and its application in biomedical and healthcare fields.

Data availability statement

The original contributions presented in the study are included in the article/supplementary material, further inquiries can be directed to the corresponding authors.

Author contributions

PD performed the experiment and wrote the whole manuscript in addition to data curation, and formal analysis. HD, HK, SA, and VY edited the manuscript and helped with revision, software, interpretation and formal analysis. VD performed investigation, original draft writing, project administration, validation, visualization and also contributed to critically analyzing the manuscript and final approval of the version for publication. AP and HD helped in editing, project administration, methodology, investigation and funding acquisition. All authors contributed to the article and approved the submitted version.

Acknowledgments

This research was supported by Researchers Supporting Project number (RSP2023R27), King Saud University, Riyadh, Saudi Arabia. This research work is supported by "CURIE Core Grants for Women Universities, "Dated 23 January 2023, File No.: DST/CURIE-01/2023/MU.

Conflict of interest

The authors declare that the research was conducted in the absence of any commercial or financial relationships that could be construed as a potential conflict of interest.

Publisher's note

All claims expressed in this article are solely those of the authors and do not necessarily represent those of their affiliated organizations, or those of the publisher, the editors and the reviewers. Any product that may be evaluated in this article, or claim that may be made by its manufacturer, is not guaranteed or endorsed by the publisher.

RETRACTED

References

Adjiri, A. (2016). Identifying and targeting the cause of cancer is needed to cure cancer. *Oncol. Ther.* 4, 17–33. doi:10.1007/s40487-015-0015-6

Akintelu, S. A., Folorunso, A. S., Folorunso, F. A., and Oyebamiji, A. K. (2020). Green synthesis of copper oxide nanoparticles for biomedical application and environmental remediation. *Heliyon* 6, e04508. doi:10.1016/j.heliyon.2020.e04508

Almutairi, B., Albahser, G., Almeer, R., Alyami, N. M., Almukhlafi, H., Yaseen, K. N., et al. (2020). Investigation of cytotoxicity apoptotic and inflammatory responses of biosynthesized zinc oxide nanoparticles from ocimum sanctum linn in human skin keratinocyte (hacat) and human lung epithelial (A549) cells. *Oxid. Med. Cell. Longev.* 2020, 1835475. doi:10.1155/2020/1835475

Alphandéry, E. (2020). Natural metallic nanoparticles for application in nano-oncology. *Int. J. Mol. Sci.* 21, 4412–12. doi:10.3390/ijms21124412

Anand, U., Dey, A., Chandel, A. K. S., Sanyal, R., Mishra, A., Pandey, D. K., et al. (2023). Cancer chemotherapy and beyond: current status, drug candidates, associated risks and progress in targeted therapeutics. *Genes. Dis.* 10, 1367–1401. doi:10.1016/j.gendis.2022.02.007

Andualem, W. W., Sabir, F. K., Mohammed, E. T., Belay, H. H., and Gonfa, B. A. (2020). Synthesis of copper oxide nanoparticles using plant leaf extract of catha edulis and its antibacterial activity. *J. Nanotechnol.* 2020, 1–10. doi:10.1155/2020/2932434

Arakha, M., Borah, S. M., Saleem, M., Jha, A. N., and Jha, S. (2016). Interfacial assembly at silver nanoparticle enhances the antibacterial efficacy of nisin. *Free Radic. Biol. Med.* 101, 434–445. doi:10.1016/j.freeradbiomed.2016.11.016

Aranda, A., Sequedo, L., Tolosa, L., Quintas, G., Burello, E., Castell, J. V., et al. (2013). Dichloro-dihydro-fluorescein diacetate (DCFH-DA) assay: a quantitative method for oxidative stress assessment of nanoparticle-treated cells. *Toxicol. Vitro* 27, 954–963. doi:10.1016/j.tiv.2013.01.016

Asghar, M. A., Zahir, E., Asghar, M. A., Iqbal, J., and Rehman, A. A. (2020). Facile, one-pot biosynthesis and characterization of iron, copper and silver nanoparticles using Syzygium cumini leaf extract: as an effective antimicrobial and aflatoxin B1 adsorption agents. *PLoS One* 15, e0234964. doi:10.1371/journal.pone.0234964

Badrooh, M., Shokrollahi, F., Javan, S., Ghasemipour, T., Rezaei Mojdehi, S., Farahnak, H., et al. (2022). Trigger of apoptosis in adenocarcinoma gastric cell line (AGS) by a complex of thiosemicarbazone and copper nanoparticles. *Mol. Biol. Rep.* 49, 2217–2226. doi:10.1007/s11033-021-07043-z

Balram, D., Lian, K. Y., and Sebastian, N. (2023). Electrocatalytic platform based on silver-doped sugar apple-like cupric oxide embedded functionalized carbon nanotubes for nanomolar detection of acetaminophen (APAP). *Sensors* 23, 379. doi:10.3390/s23010379

Batool, M., Qureshi, Z., Mehboob, N., and Shah Abdul Salam (2018). Studie on malachite green dye degradation by biogenic metal nano cuo and cuo/zno nano composites. *Archives Nanomedicine Open Access J.* 1, 119. doi:10.32474/anoaj.2018.01.000119

Bhavana, S., Kusuma, C. G., Gubbiveeranna, V., Sumachirayu, C. K., Ravikumar, H., and Nagaraju, S. (2022). Green route synthesis of copper oxide nanoparticles using Vitex altissima [L] leaves extract and their potential anticancer activity against A549 cell lines and its apoptosis induction. *Inorg. Nano-Metal Chem.* 2022, 1–14. doi:10.1080/24701556.2022.2081195

Biresaw, S. S., and Taneja, P. (2022). Copper nanoparticles green synthesis and characterization as anticancer potential in breast cancer cells (MCF7) derived from Prunus nepalensis phytochemicals. *Mater Today Proc.* 49, 3501–3509. doi:10.1016/j.matpr.2021.07.149

Brunet, P., McGlynn, R. J., Alessi, B., Smail, F., Boies, A., Maguire, P., et al. (2021). Surfactant-free synthesis of copper nanoparticles and gas phase integration in CNT-composite materials. *Nanoscale Adv.* 3, 781–788. doi:10.1039/D0NA00922A

Burgess, J., Ferdousi, M., Gosal, D., Boon, C., Matsumoto, K., Marshall, A., et al. (2021). Chemotherapy-induced peripheral neuropathy: epidemiology, pathomechanisms and treatment. *Oncol. Ther.* 9, 385–450. doi:10.1007/s40487-021-00168-y

Carneiro, B. A., and El-Deiry, W. S. (2020). Targeting apoptosis in cancer therapy. *Nat. Rev. Clin. Oncol.* 17, 395–417. doi:10.1038/s41571-020-0341-y

Chakraborty, N., Banerjee, J., Chakraborty, P., Banerjee, A., Chanda, S., Ray, K., et al. (2022). Green synthesis of copper/copper oxide nanoparticles and their applications: A review. *Green Chem. Lett. Rev.* 15, 187–215. doi:10.1080/17518253.2022.2025916

Chandraker, S. K., Lal, M., Ghosh, M. K., Tiwari, V., Ghorai, T. K., and Shukla, R. (2020). Green synthesis of copper nanoparticles using leaf extract of Ageratum houstonianum Mill. and study of their photocatalytic and antibacterial activities. *Nano Express* 1, 010033. doi:10.1088/2632-959X/ab8e99

Chen, L., Yu, Z., and Jin, H. (2010). Comparison of ribosomal DNA ITS regions among Hippophae rhamnoides ssp. sinensis from different geographic areas in China. *Plant Mol. Biol. Rep.* 28, 635–645. doi:10.1007/s11105-010-0194-0

Chen, Z., Kankala, R. K., Yang, Z., Li, W., Xie, S., Li, H., et al. (2022). Antibody-based drug delivery systems for cancer therapy: mechanisms, challenges, and prospects. *Theranostics* 12, 3719–3746. doi:10.7150/thno.72594

Choudhary, N., Dhingra, N., Gacem, A., Yadav, V. K., Kumar Verma, R., Choudhary, M., et al. (2023). Towards further understanding the applications of endophytes: enriched source of bioactive compounds and bio factories for nanoparticles. *Front. Plant Sci.* 14, 1193573. doi:10.3389/fpls.2023.1193573

Chowdhury, D. R., Chatterjee, S. K., and Kanti Roy, S. (2016). Studies on endophytic fungi of Calotropis procera (L) R.Br. with A view to their antimicrobial and antioxidant

actvities mediated by extracellular synthesised silver nanoparticles. *IOSR J. Pharm. Biol. Sci.* 11, 113–121. doi:10.9790/3008-110502113121

Chung, I., Rahuman, A. A., Marimuthu, S., Kirthi, A. V., Anbarasan, K., Padmini, P., et al. (2017). Green synthesis of copper nanoparticles using eclipta prostrata leaves extract and their antioxidant and cytotoxic activities. *Exp. Ther. Med.* 14, 18–24. doi:10.3892/etm.2017.4466

Das, A. K., Fanan, A., Ali, D., Solanki, V. S., Pare, B., Almutairi, B. O., et al. (2022). Green synthesis of unsaturated fatty acid mediated magnetite nanoparticles and their structural and magnetic studies. *Magnetochemistry* 8, 174. doi:10.3390/magnetochemistry8120174

Din, M. I., Arshad, F., Hussain, Z., and Mukhtar, M. (2017). Green adeptness in the synthesis and stabilization of copper nanoparticles: catalytic, antibacterial, cytotoxicity, and antioxidant activities. *Nanoscale Res. Lett.* 12, 638. doi:10.1186/s11671-017-2399-8

Emima Jeronsia, J., Allwin Joseph, L., Annie Vinosha, P., Jerline Mary, A., and Jerome Das, S. (2019). Camellia sinensis leaf extract mediated synthesis of copper oxide nanostructures for potential biomedical applications. *Mater Today Proc.* 8, 214–222. doi:10.1016/j.matpr.2019.02.103

Ghosh, M. K., Sahu, S., Gupta, I., and Ghorai, T. K. (2020). Green synthesis of copper nanoparticles from an extract ofJatropha curcasleaves: characterization, optical properties, CT-DNA binding and photocatalytic activity. *RSC Adv.* 10, 22027–22035. doi:10.1039/d0ra03186k

Gnanavel, V., Palanichamy, V., and Roopan, S. M. (2017). Biosynthesis and characterization of copper oxide nanoparticles and its anticancer activity on human colon cancer cell lines (HCT-116). *J. Photochem Photobiol. B* 171, 133–138. doi:10.1016/j.jphotobiol.2017.05.001

Gobane, S., Dama, T., Hasan, N., and Yanmaz, E. (2023). Characterization of copper oxide-jatropha oil nanofluid as a secondary refrigerant. *J. Nanomater* 2023, 1–7. doi:10.1155/2023/7612959

Gomathi, A. C., Xavier Rajarathinam, S. R., Mohammed Sadiq, A., and Rajeshkumar, S. (2020). Anticancer activity of silver nanoparticles synthesized using aqueous fruit shell extract of *Tamarindus indica* on MCF-7 human breast cancer cell line. *J. Drug Deliv. Sci. Technol.* 55, 101376. doi:10.1016/j.jddst.2019.101376

Gu, H., Chen, X., Chen, F., Zhou, X., and Parsaee, Z. (2018). Ultrasound-assisted biosynthesis of CuO-NPs using brown alga Cystoseira trinodis: characterization, photocatalytic AOP, DPPH scavenging and antibacterial investigations. *Ultrason. Sonochem* 41, 109–119. doi:10.1016/j.ultsonch.2017.09.006

Halbus, A. F., Horozov, T. S., and Paunov, V. N. (2019). Strongly enhanced antibacterial action of copper oxide nanoparticles with boronic acid surface functionality. *ACS Appl. Mater Interfaces* 11, 12232–12243. doi:10.1021/acsami.8b21862

Hashemi, Z., Mizwari, Z. M., Mohammadi-Aghdam, S., Mortazavi-Derazkola, S., and Ali Ebrahimzadeh, M. (2022). Sustainable green synthesis of silver nanoparticles using Sambucus ebulus phenolic extract (AgNPs@SEE): optimization and assessment of photocatalytic degradation of methyl orange and their *in vitro* antibacterial and anticancer activity. *Arabian J. Chem.* 15, 103525. doi:10.1016/j.arabjc.2021.103525

Hua, H., Zhang, H., Chen, J., Wang, J., Liu, J., and Jiang, Y. (2021). Targeting Akt in cancer for precision therapy. *J. Hematol. Oncol.* 14, 128. doi:10.1186/s13045-021-01137-8

Huang, Y., Li, P., Zhao, R., Zhao, L., Liu, J., Peng, S., et al. (2022). Silica nanoparticles: biomedical applications and toxicity. *Biomed. Pharmacother.* 151, 113053. doi:10.1016/j.biopha.2022.113053

Iliger, K. S., Sofi, T. A., Bhat, N. A., Ahanger, F. A., Sekhar, J. C., Elhendi, A. Z., et al. (2021). Copper nanoparticles: green synthesis and managing fruit rot disease of chilli caused by Colletotrichum capsici. *Saudi J. Biol. Sci.* 28, 1477–1486. doi:10.1016/j.sjbs.2020.12.003

Imoisili, P. E., and Jen, T.-C. (2022). Microwave-assisted sol–gel template-free synthesis and characterization of silica nanoparticles obtained from South African coal fly ash. *Nanotechnol. Rev.* 11, 3042–3052. doi:10.1515/ntrev-2022-0476

Inwati, G. K., Kumar, P., Singh, M., Yadav, V. K., Kumar, A., Soma, V. R., et al. (2021). Study of photoluminescence and nonlinear optical behaviour of AgCu nanoparticles for nanophotonics. *Nano-Structures Nano-Objects* 28, 100807. doi:10.1016/j.nanoso.2021.100807

Iyer, H., Ghosh, T., Garg, A., Agarwal, H., Jain, D., Pandey, R., et al. (2023). Lung cancer in Asian Indian females: identification of disease-specific characteristics and outcome measures over a 12-year period. *Lung India* 40, 4–11. doi:10.4103/lungindia.lungindia_43_22

Jagaran, K., and Singh, M. (2021). Nanomedicine for neurodegenerative disorders: focus on alzheimer's and Parkinson's diseases. *Int. J. Mol. Sci.* 22, 9082. doi:10.3390/ijms22169082

Jana, J., Ganguly, M., and Pal, T. (2016). Enlightening surface plasmon resonance effect of metal nanoparticles for practical spectroscopic application. *RSC Adv.* 6, 86174–86211. doi:10.1039/C6RA14173K

Khan, F., Pandey, P., Ahmad, V., and Upadhyay, T. K. (2020). Moringa oleifera methanolic leaves extract induces apoptosis and G0/G1 cell cycle arrest via downregulation of Hedgehog Signaling Pathway in human prostate PC-3 cancer cells. *J. Food Biochem.* 44, e13338. doi:10.1111/jfbc.13338

Kim, H. S., and Lee, D. Y. (2022). Nanomedicine in clinical photodynamic therapy for the treatment of brain tumors. *Biomedicines* 10, 96. doi:10.3390/biomedicines10010096

Krejsa, C. M., and Schieven, G. L. (2000). "Detection of oxidative stress in lymphocytes using dichlorodihydrofluorescein diacetate," in *Stress response. Methods in molecular biology™*. Editors J. M. Walker and S. M. Keyse (Humana Press), 99. doi:10.1385/1-59259-054-3:35

Kulothungan, V., Sathishkumar, K., Leburu, S., Ramamoorthy, T., Stephen, S., Basavarajappa, D., et al. (2022). Burden of cancers in India - estimates of cancer crude incidence, YLLs, YLDs and DALYs for 2021 and 2025 based on National Cancer Registry Program. *BMC Cancer* 22, 527. doi:10.1186/s12885-022-09578-1

Kumar, I., Mondal, M., Meyappan, V., and Sakthivel, N. (2019). Green one-pot synthesis of gold nanoparticles using Sansevieria roxburghiana leaf extract for the catalytic degradation of toxic organic pollutants. *Mater Res. Bull.* 117, 18–27. doi:10.1016/j.materresbull.2019.04.029

Lee, Y. H., Jang, H. J., Park, K. H., Kim, S. H., Kim, J. K., Kim, J. C., et al. (2021). Phytochemical investigation of bioactive compounds from white kidney beans (fruits of *Phaseolus multiflorus* var. *Albus*): identification of denatonium with osteogenesis-inducing effect. *Plants* 10, 2205. doi:10.3390/plants10102205

Lin, B., Lu, L., Wang, Y., Zhang, Q., Wang, Z., Cheng, G., et al. (2021). Nanomedicine directs neuronal differentiation of neural stem cells via silencing long noncoding RNA for stroke therapy. *Nano Lett.* 21, 806–815. doi:10.1021/acs.nanolett.0c04560

Lindenboim, L., Zohar, H., Worman, H. J., and Stein, R. (2020). The nuclear envelope: target and mediator of the apoptotic process. *Cell. Death Discov.* 6, 29. doi:10.1038/s41420-020-0256-5

Loo, Y. Y., Chieng, B. W., Nishibuchi, M., and Radu, S. (2012). Synthesis of silver nanoparticles by using tea leaf extract from Camellia Sinensis. *Int. J. Nanomedicine* 7, 4263–4267. doi:10.2147/IJN.S33344

López-Santiago, C. A., Otero-Rozas, E., Martín-López, B., Plieninger, T., Martín, E. G., and González, J. A. (2014). Using visual stimuli to explore the social perceptions of ecosystem services in cultural landscapes: the case of transhumance in Mediterranean Spain. *Ecol. Soc.* 19, art27. doi:10.5751/ES-06401-190227

Loprinzi, C. L., Lacchetti, C., Bleeker, J., Cavaletti, G., Chauhan, C., Hertz, D. L., et al. (2020). Prevention and management of chemotherapy-induced peripheral neuropathy in survivors of adult cancers: ASCO guideline update. *J. Clin. Oncol.* 38, 3325–3348. doi:10.1200/JCO.20.01399

Ma, C., Zhang, Y., Hu, S., Liu, X., and He, S. (2022). A copper nanoparticle enhanced phase change material with high thermal conductivity and latent heat for battery thermal management. *J. Loss Prev. Process Ind.* 78, 104814. doi:10.1016/j.jlp.2022.104814

Ma, Q., Chen, X., Zhang, K., Yao, D., Yang, L., Wang, H., et al. (2020). Chemical fingerprint analysis for discovering markers and identifying saussurea involucrata by HPLC coupled with OPLS-DA. *J. Anal. Methods Chem.* 2020, 7560710. doi:10.1155/2020/7560710

Mali, S. C., Dhaka, A., Githala, C. K., and Trivedi, R. (2020). Green synthesis of copper nanoparticles using Celastrus paniculatus Willd. leaf extract and their photocatalytic and antifungal properties. *Biotechnol. Rep.* 27, e00518. doi:10.1016/j.btre.2020.e00518

Maliki, M., Ifijen, I. H., Ikhuoria, E. U., Jonathan, E. M., Onaiwu, G. E., Archibong, U. D., et al. (2022). Copper nanoparticles and their oxides: optical, anticancer and antibacterial properties. *Int. Nano Lett.* 12, 379–398. doi:10.1007/s40089-022-00380-2

Mallikarjunaswamy, C., Parameswara, P., Pramila, S., Nagaraju, G., Deepakumari, H. N., and Lakshmi Ranganatha, V. (2022). Green and facile synthesis of zinc oxide nanoparticles for enhanced photocatalytic organic pollutant degradation. *J. Mater. Sci. Mater. Electron.* 33, 20361–20372. doi:10.1007/s10854-022-08852-z

McBride, A. A. (2022). Human papillomaviruses: diversity, infection and host interactions. *Nat. Rev. Microbiol.* 20, 95–108. doi:10.1038/s41579-021-00617-5

Modi, S., Yadav, V. K., Amari, A., Osman, H., Igwegbe, C. A., and Fulekar, M. H. (2023). Nanobioremediation: A bacterial consortium-zinc oxide nanoparticle-based approach for the removal of methylene blue dye from wastewater. *Environ. Sci. Pollut. Res.* 30, 72641–72651. doi:10.1007/s11356-023-27507-y

Mohamed, H. I., Sajyan, T. K., Shaalan, R., Bejjani, R., Sassine, Y. N., and Basit, A. (2022). "Chapter 4 - plant-mediated copper nanoparticles for agri-ecosystem applications," in *Agri-waste and microbes for production of sustainable nanomaterials*. Editors K. A. Abd-Elsalam, R. Periakaruppan, and S. Rajeshkumar (Amsterdam, Netherlands: Elsevier), 79–120. doi:10.1016/B978-0-12-823575-1.00025-1

Mukhopadhyay, R., Kazi, J., and Debnath, M. C. (2018). Synthesis and characterization of copper nanoparticles stabilized with Quisqualis indica extract: evaluation of its cytotoxicity and apoptosis in B16F10 melanoma cells. *Biomed. Pharmacother.* 97, 1373–1385. doi:10.1016/j.biopha.2017.10.167

Mummudi, N., Agarwal, J. P., Chatterjee, S., Mallick, I., and Ghosh-Laskar, S. (2019). Oral cavity cancer in the Indian subcontinent – challenges and opportunities. *Clin. Oncol.* 31, 520–528. doi:10.1016/j.clon.2019.05.013

Nagajyothi, P. C., Muthuraman, P., Sreekanth, T. V. M., Kim, D. H., and Shim, J. (2017). Green synthesis: *in-vitro* anticancer activity of copper oxide nanoparticles against human cervical carcinoma cells. *Arabian J. Chem.* 10, 215–225. doi:10.1016/j.arabjc.2016.01.011

RETRACTED

Pareek, S., Rout, V., Jain, U., Bharadwaj, M., and Chauhan, N. (2021). Nitrogen-doped carbon dots for selective and rapid gene detection of human papillomavirus causing cervical cancer. *ACS Omega* 6, 31037–31045. doi:10.1021/acsomega.1c03919

Pariona, N., Mtz-Enriquez, A. I., Sánchez-Rangel, D., Carrión, G., Paraguay-Delgado, F., and Rosas-Saito, G. (2019). Green-synthesized copper nanoparticles as a potential antifungal against plant pathogens. *RSC Adv.* 9, 18835–18843. doi:10.1039/c9ra03110c

Pinto, T., Aires, A., Cosme, F., Bacelar, E., Morais, M. C., Oliveira, I., et al. (2021). Bioactive (Poly)phenols, volatile compounds from vegetables, medicinal and aromatic plants. *Foods* 10, 106. doi:10.3390/foods10010106

Prasad, P. R., Kanchi, S., and Naidoo, E. B. (2016). *In-vitro* evaluation of copper nanoparticles cytotoxicity on prostate cancer cell lines and their antioxidant, sensing and catalytic activity: one-pot green approach. *J. Photochem Photobiol. B* 161, 375–382. doi:10.1016/j.jphotobiol.2016.06.008

Priya, G., Verma, R. K., Lakhawat, S., Yadav, V. K., Gacem, A., Abbas, M., et al. (2023). Millets: sustainable treasure house of bioactive components. *Int. J. Food Prop.* 26, 1822–1840. doi:10.1080/10942912.2023.2236317

Pucci, C., Martinelli, C., and Ciofani, G. (2019). Innovative approaches for cancer treatment: current perspectives and new challenges. *Ecancermedicalscience* 13, 961. doi:10.3332/ecancer.2019.961

Pugazhendhi, A., Prabhu, R., Muruganantham, K., Shanmuganathan, R., and Natarajan, S. (2019). Anticancer, antimicrobial and photocatalytic activities of green synthesized magnesium oxide nanoparticles (MgONPs) using aqueous extract of Sargassum wightii. *J. Photochem Photobiol. B* 190, 86–97. doi:10.1016/j.jphotobiol.2018.11.014

Pundir, S., Garg, P., Dviwedi, A., Ali, A., Kapoor, V. K., Kapoor, D., et al. (2021). Ethnomedicinal uses, phytochemistry and dermatological effects of Hippophae rhamnoides L.: A review. *J. Ethnopharmacol.* 266, 113434. doi:10.1016/j.jep.2020.113434

Radhakrishnan, R., Khan, F. L. A., Muthu, A., Manokaran, A., Savarenathan, J. S., and Kasinathan, K. (2021). Green synthesis of copper oxide nanoparticles mediated by aqueous leaf extracts of leucas aspera and Morinda tinctoria. *Lett. Appl. NanoBioScience* 10, 2706–2714. doi:10.33263/lianbs104.27062714

Rashtbari, Y., Sher, F., Afshin, S., Hamzezadeh, A., Ahmadi, S., Azhar, O., et al. (2022). Green synthesis of zero-valent iron nanoparticles and loading effect on activated carbon for furfural adsorption. *Chemosphere* 287, 132114. doi:10.1016/j.chemosphere.2021.132114

Ray, S. S., and Bandyopadhyay, J. (2021). Nanotechnology-enabled biomedical engineering: current trends, future scopes, and perspectives, *Nanotechnol. Rev.* 10, 728–743. doi:10.1515/ntrev-2021-0052

Rhaman, M. M., Islam, M. R., Akash, S., Mim, M., Noor alam, M., Nepovimova, E., et al. (2022). Exploring the role of nanomedicines for the therapeutic approach of central nervous system dysfunction: at a glance. *Front. Cell. Dev. Biol.* 10, 989471. doi:10.3389/fcell.2022.989471

Riley, R. S., June, C. H., Langer, R., and Mitchell, M. J. (2019). Delivery technologies for cancer immunotherapy. *Nat. Rev. Drug Discov.* 18, 175–196. doi:10.1038/s41573-018-0006-z

Roy, A., Basuthakur, P., and Patra, C. R. (2021). "Therapeutic applications of noble metal (Au, Ag, Pt)-Based nanomedicines for melanoma," in *Nanomedicine for cancer diagnosis and therapy*. Editors A. Malik, S. Afaq, and M. Tarique (Singapore: Springer Singapore), 161–202. doi:10.1007/978-981-15-7564-8_8

Sagadevan, S., Imteyaz, S., Murugan, B., Anita Lett, J., Sridewi, N., Weldegebrieal, G. K., et al. (2022). A comprehensive review on green synthesis of titanium dioxide nanoparticles and their diverse biomedical applications. *Green Process. Synthesis* 11, 44–63. doi:10.1515/gps-2022-0005

Sánchez-López, E., Gomes, D., Esteruelas, G., Bonilla, L., Lopez-Machado, A. L., Galindo, R., et al. (2020). Metal-based nanoparticles as antimicrobial agents: an overview. *Nanomaterials* 10, 292. doi:10.3390/nano10020292

Sathishkumar, K., Chaturvedi, M., Das, P., Stephen, S., and Mathur, P. (2022). Cancer incidence estimates for 2022 and projection for 2025: result from national cancer registry programme, India. *Indian J. Med. Res.* 156, 598–607. doi:10.4103/ijmr.ijmr_1821_22

Schlottmann, F., Casas, M. A., and Molena, D. (2022). Evidence-based approach to the treatment of esophagogastric junction tumors. *World J. Clin. Oncol.* 13 (3), 159–167. doi:10.5306/wjco.v13.i3.159

Sebastian, N., Yu, W. C., and Balram, D. (2022). Ultrasensitive electrochemical detection and plasmon-enhanced photocatalytic degradation of rhodamine B based on dual-functional, 3D, hierarchical Ag/ZnO nanoflowers. *Sensors* 22, 5049. doi:10.3390/s22135049

Shafiei, I., Tavassoli, S. P., Rahmatollahi, H. R., Ghasemian, R., and Salehzadeh, A. (2022). A novel copper oxide nanoparticle conjugated by thiosemicarbazone promote apoptosis in human breast cancer cell line. *J. Clust. Sci.* 33, 2697–2706. doi:10.1007/s10876-021-02187-1

Shen, N., Wang, T., Gan, Q., Liu, S., Wang, L., and Jin, B. (2022). Plant flavonoids: classification, distribution, biosynthesis, and antioxidant activity. *Food Chem.* 383, 132531. doi:10.1016/j.foodchem.2022.132531

Siddiqui, V. U., Ansari, A., Chauhan, R., and Siddiqi, W. A. (2021). Green synthesis of copper oxide (CuO) nanoparticles by Punica granatum peel extract. *Mater Today Proc.* 36, 751–755. doi:10.1016/j.matpr.2020.05.504

Singh Jassal, P., Kaur, D., Prasad, R., and Singh, J. (2022). Green synthesis of titanium dioxide nanoparticles: development and applications. *J. Agric. Food Res.* 10, 100361. doi:10.1016/j.jafr.2022.100361

Sivaraj, R., Rahman, P. K. S. M., Rajiv, P., Narendhran, S., and Venckatesh, R. (2014). Biosynthesis and characterization of Acalypha indica mediated copper oxide nanoparticles and evaluation of its antimicrobial and anticancer activity. *Spectrochim. Acta A Mol. Biomol. Spectrosc.* 129, 255–258. doi:10.1016/j.saa.2014.03.027

Tirichen, H., Yaigoub, H., Xu, W., Wu, C., Li, R., and Li, Y. (2021). Mitochondrial reactive oxygen species and their contribution in chronic kidney disease progression through oxidative stress. *Front. Physiol.* 12, 627837. doi:10.3389/fphys.2021.627837

Tuli, H. S., Joshi, R., Kaur, G., Garg, V. K., Sak, K., Varol, M., et al. (2023). Metal nanoparticles in cancer: from synthesis and metabolism to cellular interactions. *J. Nanostructure Chem.* 13, 321–348. doi:10.1007/s40097-022-00504-2

Vasanth, K., Ilango, K., MohanKumar, R., Agrawal, A., and Dubey, G. P. (2014). Anticancer activity of Moringa oleifera mediated silver nanoparticles on human cervical carcinoma cells by apoptosis induction. *Colloids Surf. B Biointerfaces* 117, 354–359. doi:10.1016/j.colsurfb.2014.02.052

Vinita and Punia, D. (2018). Seabuckthorn: A potential medicinal shrub. *Int. J. Chem. Stud.* 6, 1804–1811.

Vishnu, S., Ramaswamy, P., Narendhran, S., and Sivaraj, R. (2016). Potentiating effect of ecofriendly synthesis of copper oxide nanoparticles using brown alga: antimicrobial and anticancer activities. *Bull. Mater. Sci.* 39, 361–364. doi:10.1007/s12034-016-1173-3

Wang, Z., Zhao, F., Wei, P., Chai, X., Hou, G., and Meng, Q. (2022). Phytochemistry, health benefits, and food applications of sea buckthorn (Hippophae rhamnoides L): A comprehensive review. *Front. Nutr.* 9, 1111880. doi:10.3389/fnut.2022.1111880

Waris, A., Din, M., Ali, A., Ali, M., Afridi, S., Baset, A., et al. (2021). A comprehensive review of green synthesis of copper oxide nanoparticles and their diverse biomedical applications. *Inorg. Chem. Commun.* 123, 108369. doi:10.1016/j.inoche.2020.108369

Wu, S., Rajeshkumar, S., Madasamy, M., and Mahendran, V. (2020). Green synthesis of copper nanoparticles using Cissus vitiginea and its antioxidant and antibacterial activity against urinary tract infection pathogens. *Artif. Cells Nanomed Biotechnol.* 48, 1153–1158. doi:10.1080/21691401.2020.1817053

Yadav, V. K., Ali, D., Khan, S. H., Gnanamoorthy, G., Choudhary, N., Yadav, K. K., et al. (2020). Synthesis and characterization of amorphous iron oxide nanoparticles by the sonochemical method and their application for the remediation of heavy metals from wastewater. *Nanomaterials* 10, 1551. doi:10.3390/nano10081551

Zhang, G., Yuan, C., and Sun, Y. (2018). Effect of selective encapsulation of hydroxypropyl-β-cyclodextrin on components and antibacterial properties of star anise essential oil. *Molecules* 23, 1126. doi:10.3390/molecules23051126

Zhang, W., Oraiqat, I., Litzenberg, D., Chang, K. W., Hadley, S., Sunbul, N. B., et al. (2023). Real-time, volumetric imaging of radiation dose delivery deep into the liver during cancer treatment. *Nat. Biotechnol.* doi:10.1038/s41587-022-01593-8

RETRACTED